

40. PROBABILISTIC ZONATION OF EARLY CRETACEOUS MICROFOSSIL SEQUENCES, ATLANTIC AND INDIAN OCEANS, WITH SPECIAL REFERENCE TO LEG 123¹

Felix M. Gradstein,^{2,3} Zehui Huang,³ Doug Merrett,³ and James G. Ogg⁴

ABSTRACT

A database was built of 378 stratigraphic events, including first and last stratigraphic occurrences (FO/LO) of calcareous nannofossils, foraminifers, and dinocysts, and geomagnetic reversal occurrences in Latest Jurassic through Early Cretaceous deep-marine strata of 10 Atlantic and three Indian Ocean drilling sites. A total 136 different events are included, about one-third of which are unique to either ocean; however, this number may decrease when more Indian Ocean ODP sites become available for study. Using the complete data set, with the quantitative stratigraphy methods STRATCOR and RASC, we calculated closely comparable optimum sequences of average first and last occurrence positions. The preferred zonal solution, based on the STRATCOR method, includes 56 events, each of which occurs in 3 or more sites and comprises 6 geomagnetic reversal events, 25 nannofossils, 5 planktonic and 8 benthic foraminifers, and 12 dinocysts. Eight assemblage zones of Tithonian through Albian age have been recognized that correlate most of these sites. The nannofossil events, *Crucicellipsis cuvilli* FO, *Tubodiscus verenae* FO, *Reticulolithus wisei* LO, and *Chiastozygus litterarius* FO, in the Atlantic Ocean are half a stage or more older than those in the Indian Ocean. Stratigraphic ranges of the benthic foraminifers *Haplophragmium inconstans*, *Trochammina quinqueloba*, and *Dorothyia praealtaeriviana*, differ significantly among sites. The same is true for the dinocyst events *Phoberocysta neocomica* LO and *Druggidium apicopaucicum* LO, rendering these taxa less useful for zonation and correlation.

INTRODUCTION

We propose a quantitative zonation using nannofossil, foraminifer, dinocyst, and geomagnetic reversal events in Uppermost Jurassic and Lower Cretaceous sediments in 10 Atlantic and 3 Indian Ocean sites. Indian Ocean sites are from DSDP Leg 27 and from ODP Leg 123, which had as one objective the study of Mesozoic biostratigraphy and biochronology in relation to the Atlantic oceanic record.

Conventional biostratigraphy generally lacks direct integration between individual microfossil disciplines before building a multiple zonation and rarely gives insight in the actual geographic distributions of taxa and zones. To a great extent, this is a result of the considerable regional diversity of the microfossil record, the degree of specialization needed to "digest" data from any one microfossil group, such as coccolithophorids, benthic foraminifers, and dinocysts, and the lack of standardized recording and retrieval procedures in stratigraphic paleontology. In addition, conventional qualitative methods are poorly suited for integrating records prior to zonation. For the ultimate in conventional stratigraphic resolution, considerable emphasis is placed on the end-points of (micro) fossil ranges in key sections. Unfortunately, few sites provide consistent order and presence of all "zonal" or "index" taxa proposed, which leads to considerable subjective judgment on the part of individual scientists regarding zonation, based on the perceived "true" order of taxa.

Modern quantitative zonation and correlation techniques provide a means for calculating average or total stratigraphic ranges for a variety of fossil taxa in one integrated and more objective

zonation. If average ranges are one's objective, then the procedure treats local inconsistencies in relative position of the end-points of ranges (first and last occurrence events) as local, random deviations from estimated average event locations. Using error bars, uncertainty may be exposed in the total stratigraphic ranges of taxa. Estimates of errors emphasize the probabilistic, rather than deterministic, nature of stratigraphic solutions. In this manner, debate about a so-called "true" zonation is circumvented. If total stratigraphic ranges are one's objective, as with qualitative, deterministic biostratigraphic methodology, then stratigraphic inconsistencies are assumed to result from missing data and are eliminated by filling in the data gaps, until a consistent database is obtained. Probabilistic techniques can be used to calculate usable zonations in noisy data sets that contain many sites and are suitable for groups of fossils, where a large deviation occurs between local and average stratigraphic ranges, as with many benthic organisms.

Quantitative techniques allow one to calculate integrated zonations and their correlations quickly and easily, once the data have been standardized. The process is iterative between interim answers and data, such that taxonomic bias, stratigraphic outliers, and absence of stratigraphic and taxonomic communality among sites may be quickly identified. Next, corrective measures may be taken to optimize zonations using "filtered" data, much like step-wise filtering of geophysical data during processing.

The richness of stratigraphic data in DSDP and ODP holes varies with location, determined by depositional conditions and the degree of diagenetic alteration. Studies of these data have given insight into Jurassic and Early Cretaceous stratigraphy, but most previous stratigraphic research was performed either independently on the basis of a certain fossil group among several holes (Habib, 1977, 1982) or on the basis of several fossil groups in one or two drilling sites in the form of a stratigraphic summary of a drilling leg. Jansa et al. (1979) and Ogg (1987) were the first to use various groups of fossils (nannofossils, dinoflagellates, and ammonites) and geomagnetic polarity to correlate holes (e.g., DSDP Holes 534A and 603B). Gradstein (1986) synthesized empirically Mesozoic biozonations of various fossil groups in the northwestern Atlantic Ocean.

¹ Gradstein, F. M., Ludden, J. N., et al., 1992. Proc. ODP, Sci. Results, 123: College Station, TX (Ocean Drilling Program).

² Atlantic Geoscience Centre, Bedford Institute of Oceanography, Dartmouth, Nova Scotia B2Y 4A2, Canada.

³ Department of Geology, Dalhousie University, Halifax, Nova Scotia B3H 3J5, Canada.

⁴ Department of Earth and Atmospheric Sciences, Purdue University, West Lafayette, IN 47907, U.S.A.

For a more comprehensive understanding of deep-water Mesozoic biostratigraphy, one must draw on as much information from various stratigraphic disciplines (foraminifers, nannofossils, dinoflagellates, geomagnetic polarity) as possible, preferably in a quantitative way. The stratigraphy developed on the basis of a certain fossil group in a single hole or a small area almost always suffers from redeposition and diagenetic alteration (dissolution), and sometimes misidentification. This stratigraphy may not be complete and representative enough because of diachroneity of some species.

Here, we use quantitative methods to process stratigraphic data (foraminifers, nannofossils, dinoflagellates, geomagnetic polarity) collected from 10 DSDP holes in the Atlantic Ocean (Fig. 1). We compare the Atlantic optimum stratigraphic record to that from two recently completed sites during Leg 123 in the Indian Ocean (Fig. 2) and a nearby DSDP Leg 27 site, to assess direct correlation among sites. The ODP database of 13 sites contains both pelagic and benthic fossils and has "missing" data, the reason why a probabilistic approach was preferred. Further study will be warranted to refine these zonations, using a deterministic pathway in the methods presented.

In the quantitative approach, two methods are used to calculate optimum biozonations. The first method is based on the F77 program STRATCOR, which is a crossplotting method for analyzing hole or outcrop data in succession, so as to build a composite sequence of events. The second method is the F77 program RASC, which uses matrix permutation on frequency of event occurrences to subject all data simultaneously to biostratigraphic sequence analysis. Both methods are summarized here. One of the results from STRATCOR is referred to as the Final Composite Standard Sequence (FCSS), which is expressed either as a listing or as a dendrogram of interevent distances in relative time. Both methods present more direct and more objective insights in the stratigraphic use of different fossil groups and geomagnetic reversal events than conventionally constructed zonations.

METHODS

Graphic correlation, also called Shaw's method, was proposed by Shaw (1964) and has become accepted and used by stratigraphers since that time as a semi-objective tool to assess the fossil record for purposes of zonation and correlation. This is actually a type of "crossplotting" method, where one compares order with spacing of stratigraphic events in pairs of sections, using *x-y* scatter plots. In this comparison, one section is considered the reference, while other sections are used one by one for updating data of the reference section to produce a composite sequence. The line of correlation (LOC) is derived either from subjectively

connecting events in two-way scattergrams, or from a statistically modeled line of the scattered points. Traditionally, stratigraphers have used either single straight lines or segmented straight lines as LOCs. Miller (1977) and Edwards (1989) gave good accounts of the history and use of this relatively simple, but stratigraphically useful and consistently popular, method.

For more efficient use of graphic correlation, this method has now been extensively modified and computerized for use with personal computers having graphics cards and a mathematical co-processor. This F77 program, named STRATCOR (version 2.0; Gradstein, 1990), performs both biozonation and correlation of fossil events in sedimentary strata. Examples of fossil events are the first or last occurrences of taxa in samples from holes or outcrop sections (i.e., the local stratigraphic range end-points). This method allows one to calculate a zonation, even if some events in the database occur in only a few sequences. In comparison with another quantitative technique, RASC (see below), whose results rely more on the occurrence frequency of the events in the database, STRATCOR is a more suitable tool for dealing with our smaller and more patchy data (see "Data," section, this chapter).

The program STRATCOR executes in two stages. During Stage 1, all hole sequences are incorporated in succession to form a Final Composite Standard Sequence (FCSS). During Stage 2, the FCSS is correlated with individual holes.

In detail, the method proceeds as follows: first, events in an assigned reference hole (number 1 for the program and the dependent variable) are expressed as a function of the events in common with hole number 2 (the independent variable). During Stage 1, only order of events is used in the event (hole) sequences, not their depths in feet or meters. Thus, event sequences have no scale, only an order. A best-fit line is constructed for the scattergram of events in common using cubic spline fitting. Thus, the LOC built into this program is a curved, smooth line. The program automatically calculates three smoothed spline fits:

1. A minimally smoothed fit, such that deviation to all points is minimized, but such that the curve remains monotonic (i.e., always shows positive increases in both *x* and *y* directions and does not return on itself, which creates a geologically impossible negative sedimentation rate).

2. Maximum smoothing, which is a linear regression line.

3. The average of the two previous cubic spline fits.

In addition, the user may select his own smoothing factor, as long as it is monotonic; user-controlled weights on event positions may "steer" the fit, such that it is stratigraphically most satisfac-

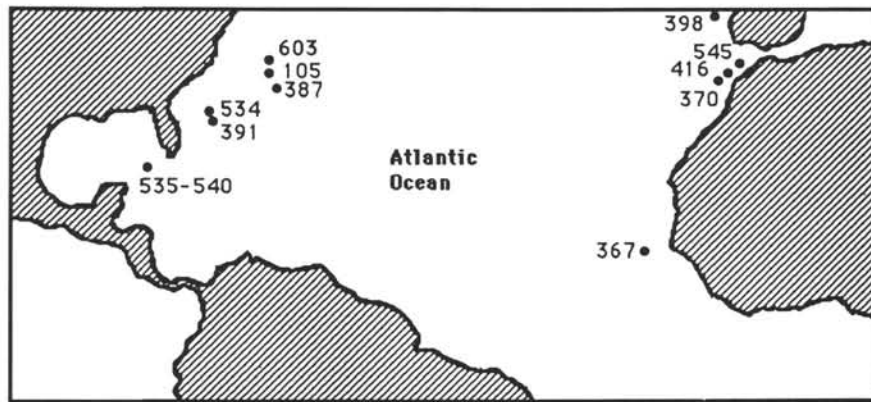


Figure 1. Location of 10 Atlantic Ocean sites that were cored during DSDP Legs 11, 41, 43, 44, 48A, 50, 76, 77, and 93.

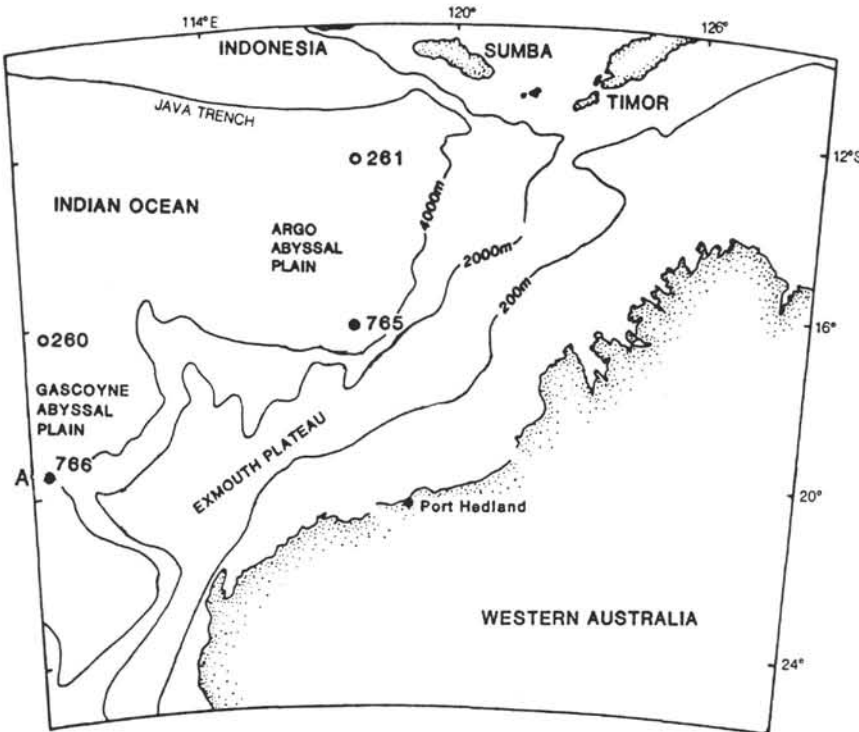


Figure 2. Location of three Indian Ocean sites that were cored during DSDP Leg 27 and ODP Leg 123.

tory and, for example, models a hiatus in a hole. In general, minimum smoothing is the preferred option, because the LOC stays nearest the observed data points, and two-way deviations from the LOC to the data points are minimized.

Events not previously in the reference hole are added at their interpolated positions. When an event in the reference hole also occurs in the individual hole, it has an interpolated position in the reference section. At this stage, the user may select one of the following stratigraphic rules to calculate the newly interpolated position in the reference hole (interim composite standard). The new position may be (1) the highest, (2) the lowest, (3) the unweighted average, or (4) the weighted average of the previous and interpolated positions in the reference hole (Fig. 3). The first two interpolation methods, Methods 1 and 2, lead to deterministic zonations, Methods 3 and 4 create probabilistic ones.

Following the interpolation of Hole 2 in Hole 1, the order of the individual record in Hole 3 is crossplotted with the previous composite, upon which interpolation again updates this composite record, and so on. The final composite standard sequence (FCSS) uses the individual stratigraphic record in all holes or outcrop sections. Stage 1 can be repeated up to 99 times, if necessary, for stabilizing the FCSS. Note that the first and last occurrence events in the FCSS are spaced along a relative stratigraphic scale that is a composite of all order relationships in all holes examined.

During Stage 2, the correlation stage of STRATCOR, the FCSS again is crossplotted with the fossil record in each individual hole, now expressed in the original depth units of measurements. Again, the composite is expressed as a function of the individual record, using cubic smoothing splines, but now the composite is interpolated in each hole to find the local depth of each composite event. The resulting correlation framework serves to draw detailed cross sections among holes or outcrop sections.

Program STRATCOR consists of three interactive modules: PREP.EXE, GRACOR.EXE, and DENDRO.EXE. The first module is a pre-processor of input data, which conform to the so-called RASC/CASC format (see below; i.e., event dictionary file, event-

sequence file, and event-depth file). PREP converts the RASC/CASC-type input data to the input format of GRACOR. More importantly, it permits the user (1) to set a threshold for minimum event occurrence, (2) to include rare events, and (3) to determine the order in which the holes or outcrop sections are processed interactively in GRACOR. GRACOR is the main program; it calculates a probabilistic or deterministic biozonation, depending on the choice of interpolation rule, and correlates the zonation through the holes. Program DENDRO displays the FCSS in dendrogram format to visualize interval or assemblage zones.

Program STRATCOR works well with both small and patchy data files that 3 to 10 holes, or with files based on dozens of holes and hundreds of taxa. In contrast, program RASC (Ranking and Scaling), developed by F. P. Agterberg and F. M. Gradstein (Gradstein et al., 1985; Agterberg et al., 1989; Agterberg, 1990), handles all event data simultaneously in large matrixes that are subject to permutations to organize the event data in an optimum sequence. The RASC method both ranks and scales biostratigraphic events in relative time. We did not attempt scaling as it generally requires larger data files and appears more suitable for benthic organisms having some inconsistencies in event order among holes than for (calcareous) planktonic organisms that form relatively consistent order in relative time among sites. The ranking method can be used with only 10 holes, if reasonable overlap in stratigraphic sequences exists, as is the case here. The result of ranking is a so-called Optimum Sequence that provides insight about the most likely order of the stratigraphic first and last occurrence events. As we will see, the FCSS from STRATCOR and the Optimum Sequence based on RASC show excellent stratigraphic convergence, which confirms the stratigraphic value of the zonal solutions.

DATA

Data for this investigation are from 10 DSDP sites in the Atlantic Ocean and 1 DSDP site and 2 ODP sites in the eastern Indian Ocean (Figs. 1, 2). All sites, except Site 387, Hole 398D,

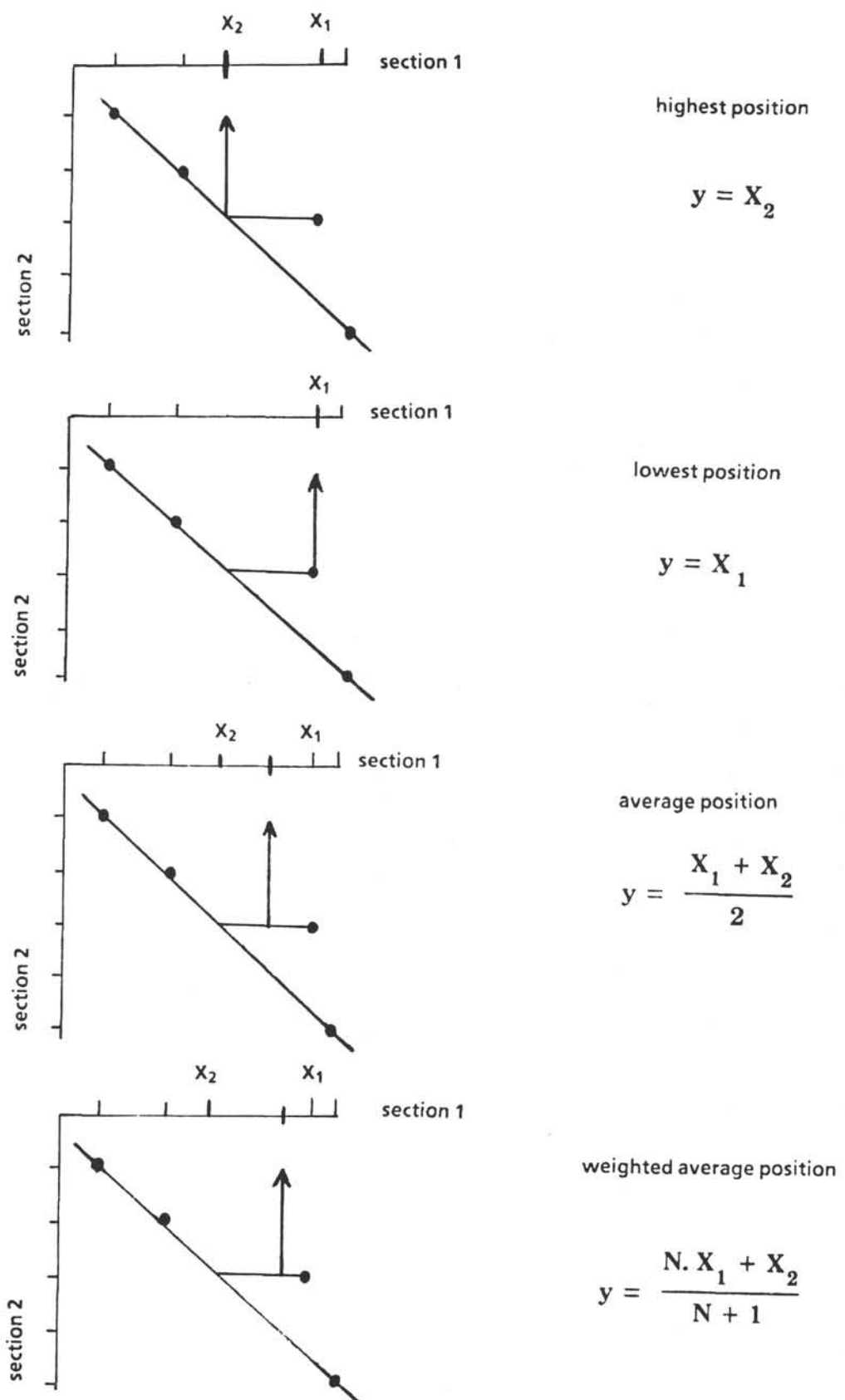


Figure 3. Four methods of stratigraphic interpolation, using smoothing cubic spline fitting in the crossplot method STRATCOR for biozonation and correlation.

and Site 766, bottomed in Jurassic oceanic basement and were already below a water depth of 4 km during the Early Cretaceous. Site 387 and Hole 398D originated in Earliest Cretaceous time and were in a paleowater depth of between 2.7 and 4 km (Jansa et al., 1979). Site 766, located on volcanic sills of Chron M11 age at the northwestern Australian ocean/continent boundary, was less than 1500 m deep during Early Cretaceous time (Ludden, Gradstein, et al., 1990).

The stratigraphic events included in this study are the first occurrence (FO) and/or last occurrence (LO) of important planktonic (PF) and benthic (BF) foraminifers, nannofossils (N) and dinoflagellates (P), which are often observed and commonly considered for stratigraphy of individual holes, and geomagnetic reversal events (M). We did not include rare fossil groups, such as ammonites and ostracods, and also excluded radiolarians and calpionellids because of an absence of systematic data among all sites examined. Once such data are available, it should be an easy matter to add and recalculate the zonations and correlations.

The data were collected mainly from research papers in relevant DSDP and ODP *Initial Reports* volumes and in other publications. The quantity and quality of stratigraphic data vary from hole to hole for various reasons. Apart from geological factors, such as depositional conditions and diagenetic process, coring interval, core recovery, and sampling density are the major factors determining the quantity and quality of the data from these holes. Detailed geomagnetic polarity study is limited to DSDP Holes 534A and 603B (Ogg, 1983, 1987). Important foraminifers

(planktonic and benthic) are sparse in most of these holes, mainly because of dissolution and difficulties when separating the fossils from the calcareous host rock. Calcareous nannofossil data are more abundant and dominate our database. Systematic studies about dinoflagellates were conducted for DSDP Holes 105, 387, 391, 534A and 603B (Habib, 1972, 1978, 1979; Habib and Drugg, 1983, 1987). More stratigraphically useful data can be found in the western Atlantic Ocean than in the eastern Atlantic or Indian oceans.

The form of data presentation in the examined published research papers varies from tabulated fossil examination results to species range charts and to simply narratives in the text. The most favorable form of data presentation for our data acquisition is the tabulated fossil examination results per sample, which allow us to recognize and avoid abnormally high fossil occurrence (first or last), because of turbiditic deposits, as is the case in DSDP Holes 603B and 534A, or because of poor preservation. Fossil range charts are subject to interpretation of the researcher. Narratives about fossil occurrences in a text are more likely to introduce noise into our database. The source of our data is listed in Table 1; a so-called event dictionary, which lists the unique code number of all taxa and magnetic polarity events, appears in Appendix A, and a complete paleontological text file that lists all data used is presented in Appendix B. The sequence of the holes arranged in the master data file of Appendix B is in accordance with the abundance and quality of the data per ocean. DSDP Hole 534A has been ranked as the primary hole (reference site), not only

Table 1. Source of data used for this study.

Hole	Foraminifers	Nannofossils	Dinoflagellates	Magnetic event
105	Luterbacher (1972)	Wilcoxon (1972)	Habib (1972) Habib (1977) Habib (1977)	
367 + 370	Kuznetsova and Seibold (1978) Pflaumann and Krasheninnikov (1978) Gradstein (1978a)	Ceppek (1978)	Williams (1978)	
387	McNulty (1979)	Okada et al. (1979)	Habib (1977) Habib (1979)	
391C	Gradstein (1978b)	Schmidt (1978) Roth (1978)	Habib (1978) Habib and Knapp (1982)	
398D	Sigal (1979)	Blechschmidt (1979)		
416A	Sliter (1980)	Cepkek et al. (1980)		
534A	Gradstein (1983)	Roth (1983)	Habib et al. (1983)	Ogg (1983)
535A + 540	Silva and McNulty (1984) Sliter and Silva (1984)	Watkins and Bowdler (1984)	Riley and Fenton (1984)	
545	Leckie (1984)	Wiegang (1984)		
603B		Covington et al. (1987)	Habib et al. (1987)	Ogg (1987)
765C + 766A + 261	Kaminski et al. (this vol.)	Mutterlose (this vol.)	Helby and McMinn (this vol.)	Ogg (in press)

because it had more events, but also because it covered a longer geological time period.

A special problem was created when in several sites first and last occurrences of four taxa were anomalously close together. In Site 534, this involved *Dorothia praeauteriviana* FO and LO (BF) at 1167 and 1149 mbsf, respectively, and *Lenticulina nodosa* FO and LO (BF) at 1167 and 1149 mbsf, respectively. In Site 370, *L. nodosa* LO (BF) was recorded only one sample above *L. nodosa* FO, and the same was true for *L. barremiana* FO and LO (BF) in Site 766, and for *Tubodiscus verenae* FO and LO (N) in Site 261. Because this involved mostly benthic foraminifers suggests either (1) that the environment was favorable for their local existence for a short time only or (2) that dissolution was important part of destroying the stratigraphic range. During trial runs to calculate and compare both STRATCOR FCSS and RASC Optimum Sequence with and without this record, solutions converged most with the record of *L. nodosa* LO and *D. praeauteriviana* LO deleted altogether, and this practice was adopted. In addition, crossplots with the FCSS showed that *L. barremiana* LO in Site 766 at 275 mbsf, and *T. verenae* LO in Site 261 at 449 mbsf were outliers. Hence, this relatively unimportant information also was omitted. Should further studies indicate that such outliers are indicative of diachroneity, their use may be reinstated.

ZONAL COMPUTATION

Zonal computations proceeded in three steps. First, we calculated an FCSS, using the data of all 13 holes. Next, we compared the FCSS with the Optimum Sequence using RASC to assess method-dependent trends. Third, we compared the FCSS in 10 Atlantic holes with that in 3 Indian Ocean sites to emphasize interoceanic differences in zonation. Finally, we propose a "universal" zonation, which may be used easily for geological correlation.

Before zonal calculations, one should gain insight in the frequency distribution of the events. This exercise takes the form of inspection of several tables. The first one (Table 2) shows DSDP and ODP holes as listed in our data file (Appendix B), numbered from 1 through 13, with the number of samples (depths) per site, which varies from 13 to 56, and the number of event occurrences per site, which varies from 17 to 62. Useful information for determining which events meet or do not meet selected thresholds is given in Table 3, which shows the dictionary events and the

Table 2. Holes with number of samples (depths) and number of stratigraphic events per site.

Hole number	Number of		Hole name
	depths	occurrences	
1	56	62	534A
2	45	46	603B
3	29	34	391C
4	20	20	105
5	19	27	370
6	20	20	535A
7	26	28	416A
8	17	17	398D
9	13	18	367
10	15	17	387
11	34	51	765
12	15	20	766
13	13	18	261

Number of holes: 13 Number of occurrences: 378

Note: these holes were processed in the order 1, 3, 2, 4, 5, 6, 7, 8, 9, 10, 11, 13, 12, which maximizes the number of taxa in common among individual sites.

Table 3. Dictionary events and number of holes in which they occur.

Event number	Number of holes	Event number	Number of holes	Event number	Number of holes
1	1	101	1	221	1
2	2	154	8	251	5
7	8	155	13	253	6
8	5	156	4	254	3
10	2	157	7	255	5
12	2	158	2	256	5
13	2	159	6	257	6
18	1	160	6	259	8
19	1	163	4	261	4
20	4	164	1	262	3
21	1	165	5	263	3
22	1	171	4	264	3
24	4	173	4	266	4
26	1	176	5	267	1
27	1	180	1	268	1
29	1	184	5	269	1
32	1	185	7	270	1
36	3	186	3	271	1
37	1	187	3	272	1
40	2	188	10	273	1
41	2	189	7	274	1
55	7	190	4	275	1
56	1	191	1	276	1
57	1	193	3	301	2
60	3	194	2	303	2
67	3	195	5	304	2
68	3	196	4	305	2
70	1	197	2	307	3
71	4	200	2	309	4
72	1	202	2	311	2
74	5	203	4	315	2
76	3	204	5	316	2
78	2	206	4	317	3
87	2	208	3	318	2
88	4	209	2	319	1
89	2	210	2	321	3
90	2	211	2	322	2
91	1	212	2	323	3
92	1	213	2	324	2
93	1	214	2	325	3
94	1	215	1	338	2
95	1	216	1	339	2
96	2	217	1	340	2
97	2	218	1		
98	1	219	1		
100	1	220	1		

Number of holes: 13 Number of occurrences: 378

The total number of dictionary events used is 135, and the total number of occurrences of these events is 378. The numerical dictionary is presented in Appendix A.

number of holes in which they occur. This table should be used in conjunction with the numerical code dictionary in Appendix A. As may be readily determined from Table 4, the majority of events are present in a few sites only. All 135 events occur in at least one site, but only one event (the LO of the nannofossil *Crucicellipsis cuvilli*) occurs in 11 or more holes. In this study, we will demand that each event in the 13 hole zonation occur in at least three holes, which limits the data to 56 fossil species or magnetic polarity events. Stratigraphically rare, but useful, events for biochronology or correlation may be added to calculated zonations as so-called unique or special events. In essence, this method proceeds such that these special events are placed between the two most adjacent taxon events in the FCSS or Optimum Sequence that also occur in the individual holes in which these special events occur.

The order in which the sites are being processed using GRA-COR should not influence the FCSS, which is why we used more than one cycle of crossplotting. Processing first proceeded

Table 4. Distribution of dictionary events by the number of holes in which they occur.

Number of holes	Frequency of events	Cumulative frequency
13	1	1
10	1	2
8	3	5
7	4	9
6	4	13
5	10	23
4	15	38
3	18	56
2	36	92
1	43	135

All 135 events occur in at least one hole, 56 in at least three holes, and so forth; Only one event occurs in at least 11 or more sites ("Cumulative Frequency" column). The "Frequency of Events" column indicates how many taxa occur in 1, 2, 3, and so forth, holes.

with all Atlantic sites such that the number of events in common per crossplot was maximized, and then Indian Ocean sites were processed. For each cycle, this order was Sites 534, 391, 603, 105, 370, 535, 416, 367, 387, 398, 765, 261, and 766.

Because the event-sequence file includes both first and last occurrences of fossils, the weighted average position (Fig. 3D) was chosen for stratigraphic interpolation using GRACOR. For this reason, the final result of our successive crossplots is a probabilistic zonation that depicts average (first or last occurrence) event positions. When interpolating the designated composite standard sequence with events in the individual hole, event positions in the reference sequence are always based on the weighted average of the old and newly interpolated positions, and the minimum smoothing factor is always used. The spline fit with a minimum smoothing factor minimizes the deviations to all points and maximizes stratigraphic "truthfulness," which is why we prefer it for interpolation. Only in Site 367 did the minimum smoothing factor fail to calculate a best fit, possibly because of violation of monotony during inverse interpolation in the middle part of the section near 940 m, where a condensed sequence appears to exist between Chrons M10 and M11. The average smoothing factor, between the minimum and the maximum (linear best fit) worked fine for Site 367.

As mentioned, the weight of every event appearing in the crossplot can be varied from -1 (for ignoring it) to +1 (for steering the spline through it) to obtain a satisfactory LOC. In Site 370, *Hedbergella delrioensis* FO (P) is far too low stratigraphically and received a weight of -1. No other event in any other hole was weighted, because the crossplots did not reveal more obvious outliers as a result of random factors.

Events in the Atlantic sites showed tight, often fairly linearly trending scattergrams, with 12 to 32 events in common between the interim FCSS and a hole's record. Spline fitting, with the exception of Site 370, was easy and revealed no obvious hiatuses. The fit between the Atlantic FCSS (after compositing 10 sites) and ODP Site 765 in the eastern Indian Ocean showed more scatter (Fig. 4), although this was not excessive. The largest deviations are shown by the benthic foraminifers, *Haplophragmium inconstans* LO (coordinates 16–22) and *Trochammina quinqueloba* LO (coordinates 15–22), both of which occur too low; the planktonic foraminifer, *Hedbergella planispira* FO (coordinates 3–8); and the dinocyst, *Phoberocysta neocomica* LO (co-

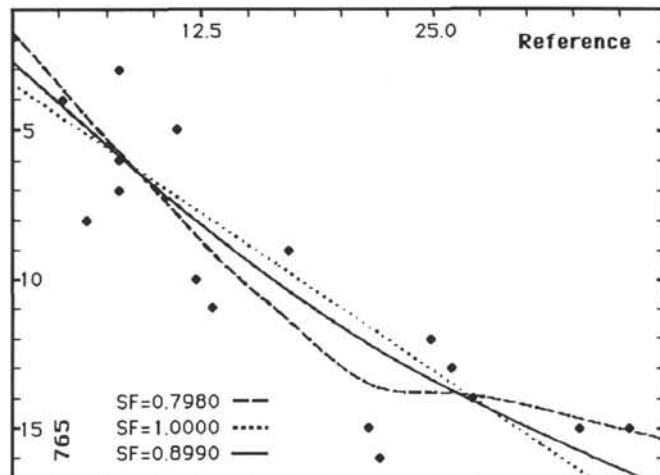


Figure 4. Crossplot of the FCSS, based on 10 Atlantic DSDP sites and the Lower Cretaceous microfossil record in Leg 123 Site 765. The cubic spline fits shown use minimum (dashed line), average (solid line), and maximum (dotted line) smoothing factors. The scale along both axes is based on the number of events per hole. For further explanation, see text.

ordinates 5–11), which occurs stratigraphically too high. Crossplots of the FCSS, including 765 with nearby Sites 261 and 766, produce tighter fits, reflecting more local coherence in order.

The process of compositing was repeated twice (3 cycles), but the differences between the FCSS in Stage 1, cycle 1 and Stage 1, cycle 2, were stratigraphically negligible. No noticeable difference could be seen between the results of cycle 2 and a third cycle 3, which is why we focused on the FCSS after two cycles.

Figure 5 (right) shows this stabilized FCSS (the results of the second cycle in Stage 1 of GRACOR) with a threshold equal to 3, and no unique events introduced. The FCSS contains the average stratigraphic position of 56 events, including 6 geomagnetic reversals, 25 nannofossils, 12 dinocysts, 8 benthic, and 5 planktonic foraminifers. Relative event ages progress from Tithonian with *Stephanolithion bigottii* LO to Albian with *Ticinella primula* FO and *Eiffellithus turriseiffeli* FO.

Figure 5 (left) shows the RASC Optimum Sequence calculated for exactly the same data and the same threshold. Correlation of the order relationship reveals remarkable convergence of stratigraphic order in both solutions. One exception is the average stratigraphic position in each zonal solution of *Haplophragmium inconstans* LO, *Trochammina quinqueloba* LO, and *Dorothia praealtaeriviana* FO, all benthic foraminifers, and to a lesser extent, *Phoberocysta neocomica* LO, *Druggidium apicopaucicum*, and *Odontochitina operculata* FO, all dinocysts. We conclude that considerable difference exists among sites in the local stratigraphic ranges of these taxa, which the RASC and STRATCOR methods, each in their own manner, do not resolve satisfactorily without additional occurrence data for these taxa from more sites. Indeed, crossplots using STRATCOR showed above average scatter for these events in some sites, as discussed earlier for the interim FCSS and ODP Site 765 (Fig. 4). Despite this scatter, the RASC and STRATCOR zonal sequences are remarkably similar, which leads us to conclude that both methods are converging on a "true" average biomagnetostratigraphic sequence of events, which may form the basis for a general zonation, as discussed next.

Another way to explore the properties of the data is to treat Indian and Atlantic sites separately, so that regional differences may be maximized. Because this creates two data sets with 10 (Atlantic) and 3 (Indian), respectively, only the STRATCOR

Sequence position	Code	Range	Events in the RASC Optimum Sequence	Events in the FCSS from STRATCOR	Code	Position	Number of wells
1	36	0-2	<i>Praeglobotruncana delrioensis</i> FO (PF)	<i>Praeglobotruncana delrioensis</i> FO (PF)	36	1.49	3
2	263	1-3	<i>Spinidinium echinoideum</i> FO (P)	<i>Spinidinium echinoideum</i> FO (P)	263	2.08	3
3	165	2-4	<i>Eiffellithus turrisieiffeli</i> FO (N)	<i>Eiffellithus turrisieiffeli</i> FO (N)	165	2.22	5
4	266	3-7	<i>Spinidinium vestitum</i> FO (P)	<i>Hedbergella delrioensis</i> FO (PF)	24	2.29	4
5	24	3-7	<i>Hedbergella delrioensis</i> FO (PF)	<i>Spinidinium vestitum</i> FO (P)	266	3.01	4
6	20	3-7	<i>Ticinella primula</i> FO (PF)	<i>Ticinella primula</i> FO (PF)	20	3.54	4
7	264	6-8	<i>Subtilisphaera perlucida</i> LO (P)	<i>Subtilisphaera perlucida</i> LO (P)	264	3.61	3
8	256	7-9	<i>Druggidium deflandrei</i> LO (P)	<i>Druggidium deflandrei</i> LO (P)	256	4.03	5
9	7	8-10	<i>Hedbergella planispira</i> FO (PF)	<i>Hedbergella planispira</i> FO (PF)	7	5.10	8
10	261	9-11	<i>Phoberocysta neocomica</i> LO (P)	<i>Hedbergella trocoidea</i> FO (PF)	8	5.11	5
11	8	10-12	<i>Hedbergella trocoidea</i> FO (PF)	<i>Rhagodiscus angustus</i> FO (N)	176	5.30	5
12	176	11-14	<i>Rhagodiscus angustus</i> FO (N)	<i>Conusphaera mexicana</i> LO (N)	195	6.09	5
13	195	10-15	<i>Conusphaera mexicana</i> LO (N)	<i>Lithastrinus floralis</i> FO (N)	193	6.45	3
14	193	12-15	<i>Lithastrinus floralis</i> FO (N)	<i>Gavelinella barremiana</i> LO (BF)	60	7.43	3
15	196	14-16	<i>Nannoconus colomii</i> LO (N)	<i>Phoberocysta neocomica</i> LO (P)	261	7.45	4
16	60	15-17	<i>Gavelinella barremiana</i> LO (BF)	<i>Nannoconus colomii</i> LO (N)	196	7.59	4
17	157	16-18	<i>Chiastozygus litterarius</i> FO (N)	<i>Chiastozygus litterarius</i> FO (N)	157	7.71	7
18	307	17-19	M3r top (M)	<i>Druggidium apicopaucicum</i> LO (P)	254	7.92	3
19	309	18-20	M4n top (M)	M4n top (M)	307	8.11	3
20	160	19-21	<i>Calcidalathina oblongata</i> LO (N)	M4n top (M)	309	8.62	4
21	187	20-22	<i>Speetonia colligata</i> LO (N)	<i>Calcidalathina oblongata</i> LO (N)	160	9.49	6
22	254	21-23	<i>Druggidium apicopaucicum</i> LO (P)	<i>Odontochitina operculata</i> FO (P)	259	10.70	8
23	155	22-24	<i>Cruciellipsis cuvillieri</i> LO (N)	<i>Speetonia colligata</i> LO (N)	187	11.49	3
24	317	23-26	M8n top (M)	M8n top (M)	317	12.03	3
25	259	23-26	<i>Odontochitina operculata</i> FO (P)	<i>Cruciellipsis cuvillieri</i> LO (N)	155	12.11	13
26	257	25-27	<i>Druggidium rhabdoreticulatum</i> FO (P)	<i>Lenticulina ouachensis</i> LO (BF)	76	13.68	3
27	321	26-28	M10n top (M)	M10n top (M)	321	14.26	3
28	76	27-30	<i>Lenticulina ouachensis</i> LO (BF)	<i>Cyclagelosphaera deflandrei</i> LO (N)	156	15.30	4
29	156	27-30	<i>Cyclagelosphaera deflandrei</i> LO (N)	<i>Druggidium rhabdoreticulatum</i> FO (P)	257	16.24	6
30	189	29-31	<i>Tubodiscus verenae</i> LO (N)	<i>Tubodiscus verenae</i> LO (N)	189	17.67	7
31	323	30-33	M10Nn top (M)	M10Nn top (M)	323	17.80	3
32	163	30-34	<i>Diadorhombus rectus</i> LO (N)	<i>Diadorhombus rectus</i> LO (N)	163	18.54	4
33	88	31-34	<i>Trochammina quinqueloba</i> LO (BF)	M11n top (M)	325	21.20	3
34	55	33-35	<i>Dorothia praehauteriviana</i> FO (BF)	<i>Scriniodinium dictyotum</i> LO (P)	262	22.16	3
35	74	34-36	<i>Lenticulina nodosa</i> FO (BF)	<i>Lenticulina nodosa</i> FO (BF)	74	22.23	5
36	325	35-37	M11n top (M)	<i>Parhabdolithus infinitus</i> FO (N)	203	23.10	4
37	203	36-38	<i>Parhabdolithus infinitus</i> FO (N)	<i>Lenticulina busanadoi</i> LO (BF)	71	23.35	4
38	262	37-39	<i>Scriniodinium dictyotum</i> LO (P)	<i>Druggidium deflandrei</i> FO (P)	255	23.72	5
39	71	38-40	<i>Lenticulina busanadoi</i> LO (BF)	<i>Dorothia praehauteriviana</i> FO (BF)	55	23.83	7
40	255	39-41	<i>Druggidium deflandrei</i> FO (P)	<i>Rucinolithus wisei</i> LO (N)	185	24.15	7
41	185	40-42	<i>Rucinolithus wisei</i> LO (N)	Trochammina quinqueloba LO (BF)	88	24.34	4
42	188	41-45	<i>Tubodiscus verenae</i> FO (N)	<i>Haplophragmium inconstans</i> LO (BF)	68	24.43	3
43	204	41-44	<i>Diadorhombus rectus</i> FO (N)	<i>Tubodiscus verenae</i> FO (N)	188	26.52	10
44	159	43-45	<i>Calcidalathina oblongata</i> FO (N)	<i>Diadorhombus rectus</i> FO (N)	204	26.84	5
45	206	44-46	<i>Reinhardtites fenestratus</i> FO (N)	<i>Calcidalathina oblongata</i> FO (N)	159	27.29	6
46	253	45-47	<i>Druggidium apicopaucicum</i> FO (P)	<i>Reinhardtites fenestratus</i> FO (N)	206	27.60	4
47	208	46-48	<i>Speetonia colligata</i> FO (N)	<i>Druggidium apicopaucicum</i> FO (P)	253	28.51	6
48	190	47-49	<i>Vagapilla stradneri</i> FO (N)	<i>Speetonia colligata</i> FO (N)	208	31.37	3
49	251	48-50	<i>Biorbitera johnnewingii</i> FO (P)	<i>Vagapilla stradneri</i> FO (N)	190	32.12	4
50	68	49-52	<i>Haplophragmium inconstans</i> LO (BF)	<i>Biorbitera johnnewingii</i> FO (P)	251	33.25	5
51	184	48-52	<i>Rucinolithus wisei</i> FO (N)	<i>Rucinolithus wisei</i> FO (N)	184	34.15	5
52	171	51-53	<i>Lithraphidites carniolensis</i> FO (N)	<i>Lithraphidites carniolensis</i> FO (N)	171	35.02	4
53	173	52-54	<i>Nannoconus colomi</i> FO (N)	<i>Cruciellipsis cuvillieri</i> FO (N)	154	36.32	8
54	186	53-55	<i>Stephanolithion bigottii</i> LO (N)	<i>Stephanolithion bigottii</i> LO (N)	186	36.65	3
55	154	54-56	<i>Cruciellipsis cuvillieri</i> FO (N)	<i>Nannoconus colomi</i> FO (N)	173	36.68	4
56	67	55-57	<i>Haplophragmium inconstans</i> FO (BF)	<i>Haplophragmium inconstans</i> FO (BF)	67	37.89	3

Figure 5. Comparison of the order of latest Jurassic and Early Cretaceous events in the Optimum Sequence using RASC, and the Final Composite Standard Sequence (FCSS) after two cycles using STRATCOR. Each first or last microfossil occurrence event or polarity reversal presence occurs in at least 3 out of 13 sites. The ordering shown is an average of all local order relationships encountered. Most crossovers are stratigraphically insignificant, with larger deviations between the two zonal solutions restricted to a few benthic foraminifers and dinocysts (e.g., the FO or LO events of the agglutinated benthic foraminifers, *Haplophragmium inconstans* and *Trochammina quinqueloba*, and the dinocysts, *Phoberocysta neocomica* and *Druggidium apicopaucicum*). This larger crossover indicates larger deviations between local and total stratigraphic ranges for these fossils, making these taxa less suitable for correlation. Nannofossils, planktonic foraminifers, and geomagnetic reversals provide the stratigraphically most stable part of the zonations. FO = first occurrence event; LO = last occurrence event; N = calcareous nannofossil; P = planktonic foraminifer; M = geomagnetic polarity reversal event; P = dinocysts (palynomorph); BF = benthic foraminifer.

method was used for zonation. RASC does not perform well with three sites, and even 10 sites is not desirable. Rather than thresholding the data severely, we stipulated that for the three Indian Ocean sites, all events must occur in at least one site (hence, no threshold), and for the 10 Atlantic sites, events must occur in a minimum of two sites. Figure 6 shows how well FCSSs correlate for the Atlantic Ocean, retaining 72 events, and the Indian Ocean sites with 66 events. Twenty-two events occur in common between the two regional biomagnetostratigraphic sequences, less than 30% of the total number of events in each solution. Hence, we conclude that a considerable number of microfossil events are unique to each group of ocean sites. This number should have been slightly less with a threshold of one for both solutions. STRATCOR satisfactorily resolves the order of the magnetic polarity chrons, and each FCSS may be considered an optimum sequence for detailed event correlation among local sites in the Tithonian–Albian time interval. Again, as in the suparegional FCSS and RASC sequences of Figure 5, the benthic foraminifers *Trochammina quinqueloba* LO and *Dorothia praealtaeriviana* FO, and the dinocyst *Phoberocysta neocomica* LO show considerable departure from stratigraphic normality among the Atlantic and Indian Ocean sites.

More systematic deviations stand out for some nannofossil events. *Cruciellipsis cuvillieri* FO appears much later in Indian (Valanginian) than Atlantic Ocean sites (Tithonian). The same is true for *Chiastozygus literarius* FO, which in the Atlantic sites is Barremian in age and Apian/Albian in the Indian Ocean sites. The FO of *Tubodiscus verenae* and the LO of *Reticularia wisei* are well below M11n (of late Valanginian age in the Atlantic, but adjacent to this chron in the Indian Ocean FCSS, possibly because of some stratigraphic condensation in the Indian Ocean sites during late Valanginian–early Hauterivian time (compare left and right sides of Fig. 7 at M10Nn–M11n positions). These observations would support migration of these taxa from the Atlantic to the Indian Ocean through time. Nevertheless, enough stratigraphic overlap exists between the two zonal sequences to warrant a single, tentative zonation based on stratigraphically average event occurrences, as proposed next. Such an approach trades the ultimate in local resolution for a more practical, generalized stratigraphic “ladder” of events.

Having established that a single FCSS may be of use for a (probabilistic) zonation of both Atlantic and Indian Ocean sites, we depict it in Figure 7. This is the FCSS of Figure 5 (right), but now displayed in dendrogram format to better express interevent distances, indicative of clustering of stratigraphic events along a relative time scale. The dendrogram includes approximately nine assemblage zones of Tithonian through Albian age, using the age connotations for the events in Ogg and Steiner (1988), Gradstein (1986), Kaminski et al. (in press), and the literature cited in Table 1. This FCSS in dendrogram format is an assemblage zonation in which different kinds of fossil and physical events have been quantitatively tied to each other. The positions of the 56 events in the FCSS represent the average stratigraphic interrelation among the events encountered in the 10 Atlantic and three Indian Ocean drilling sites.

The oldest assemblage (No. 1) contains *Stephanolithion bigotii* LO (N) of Tithonian age, and the overlying assemblage, No. 2, incorporates the FO of *Biorbifera johnnewingii* (P) and *Speetonia colligata* (N) of Berriasian age. As may be observed from Figure 6 (left), Chrons M16r and M16n occur in this zone, too (in two Atlantic sites only), and according to Ogg and Steiner (1988), are of Berriasian age. *Tubodiscus verenae* FO (N) in assemblage 3 is early Valanginian in age. The next overlying assemblage (No. 4) contains the LO of *Lenticulina busnardoii* (BF), and the FO of *Druggidium deflandrei* (P), and Chron M11n, all of late Valan-

ginian age. The overlying assemblage 5 has been assigned an early to middle Hauterivian age with the average LO of *Tubodiscus verenae* (N), the FO of *Druggidium rhabdoreticulatum* (P), the LO of *Cyclagelosphaera deflandrei* (N), and Chrons M10N and M10n. The presence of Chron M8, the LO of *Cruciellipsis cuvillieri* (N), and of *Speetonia colligata* (N) in assemblage 6 is of latest Hauterivian age. The next overlying assemblage 7 with Chrons M4n, M3r, *Calcidalathina oblongata* LO (N), and *Chiastozygus litterarius* FO (N), is Barremian in age. Assemblage zone 8 with *Rhagodiscus angustus* FO (N) and *Hedbergella trocoidea* FO (PF) is Aptian in age, and in the Atlantic FCSS of Figure 8 (left), also contains Chron M1r. The youngest assemblage zone (No. 9) includes well-known Albian events, such as *Ticinella primula* FO (PF) and *Eiffelithus turris eiffeli* FO (N).

Incorporation of many more Indian and circum North Atlantic Ocean sites will considerably refine and strengthen this tentative zonation, particularly so when less widespread, but stratigraphically significant radiolarian, cephalopod, and calpionellid data are introduced. The zonation will also provide more insight about diachroneity of events among ocean sites. With this study, we have demonstrated that quantitative processing of DSDP and ODP data leads to a practical Early Cretaceous biomagnetostratigraphic zonation. Higher resolution results when separate zonations can be calculated for each ocean basin.

ZONAL CORRELATION

Using Stage 2 of STRATCOR, the FCSS of Figure 7 may be crossplotted with the events in each individual hole, now expressed in the original depth unit of measurements (meters below seafloor). Again, the FCSS (dependent variable) is expressed as a function of the individual hole's record (independent variable), using smoothing cubic splines, but now the FCSS is interpolated in each hole to find the most likely (average) local depth of each FCSS event, even if it was not observed locally. The result is summarized in Table 5, which shows the FCSS for the Atlantic and Indian oceans (as discussed above), the measured depth of events observed in each site (Column B), and the interpolated depth of the FCSS events (Column A). Note that often only a small offset is seen between observed and interpolated (average) depths of zonal events, generally less than 10 m. In a few cases, the offset is measured in tens of meters. Blank lines in both columns indicate absence of data for executing spline crossplots between the FCSS and the individual site record.

Using the most likely age in stage units of discrete and stratigraphically reliable events in the FCSS, their interpolated depths may serve as the basis for a most likely chronostratigraphic correlation among oceanic sites. The interested user should have little trouble erecting such a scheme, using, for example, the DNAG (Kent and Gradstein, 1985) or the GTS89 (Harland et al., 1990) time scales. Conversely, the STRATCOR method applied to a much larger, and stratigraphically more refined (pelagic), data set with ammonites, radiolarians, and calpionellids represented may serve to calculate a high-resolution FCSS that can be rescaled in linear time, once enough tiepoints have been established to a standard geological time scale. Thus, a “pelagic” biochronology may be established for the Late Jurassic and Early Cretaceous time interval that can be updated readily.

SUMMARY

Detailed biostratigraphic data were accumulated during coring of Upper Jurassic and Lower Cretaceous strata in 10 Atlantic and 3 Indian Ocean sites. It is difficult to build an objective multiple biostratigraphic framework by visually comparing range charts of different fossil groups with geomagnetic reversals sequences and scattered fossil records for all 13 sites. The quantitative strati-

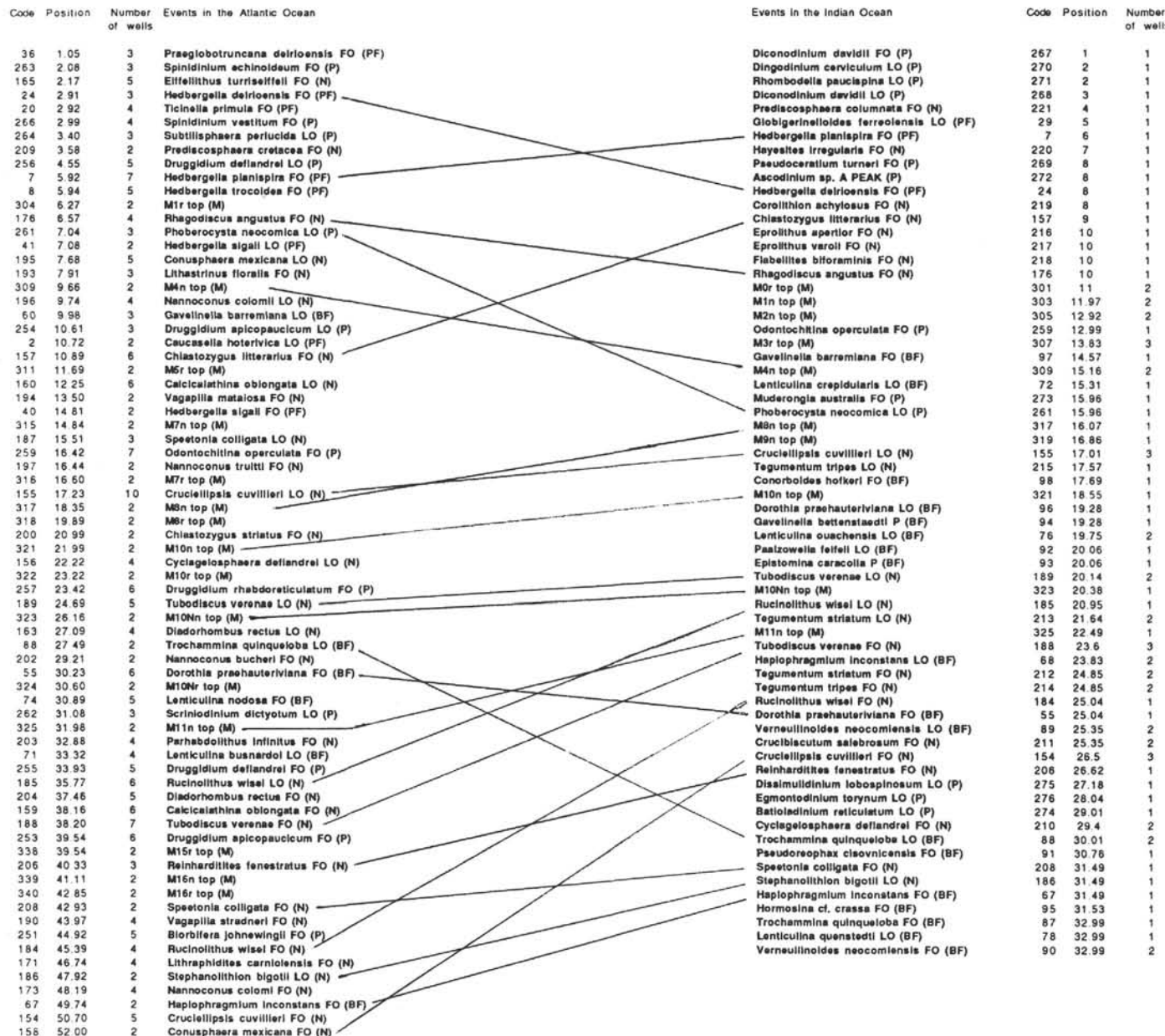


Figure 6. Comparison of the FCSS using STRATCOR for the Lower Cretaceous record in 10 Atlantic DSDP sites (left; 72 events) with the coeval record in 3 Indian Ocean ODP sites (right; 66 events). The Atlantic events occur in at least two holes. The threshold for the Indian Ocean FCSS is 1; hence, it records all events observed in any site. Twenty-two events are in common between the two zonations, with few taxa, such as the LO of the benthic foraminifer *Trochammina quinqueloba* or the dinocyst *Phoberocyysta neoconomica* showing considerable scatter.

DENDROGRAM

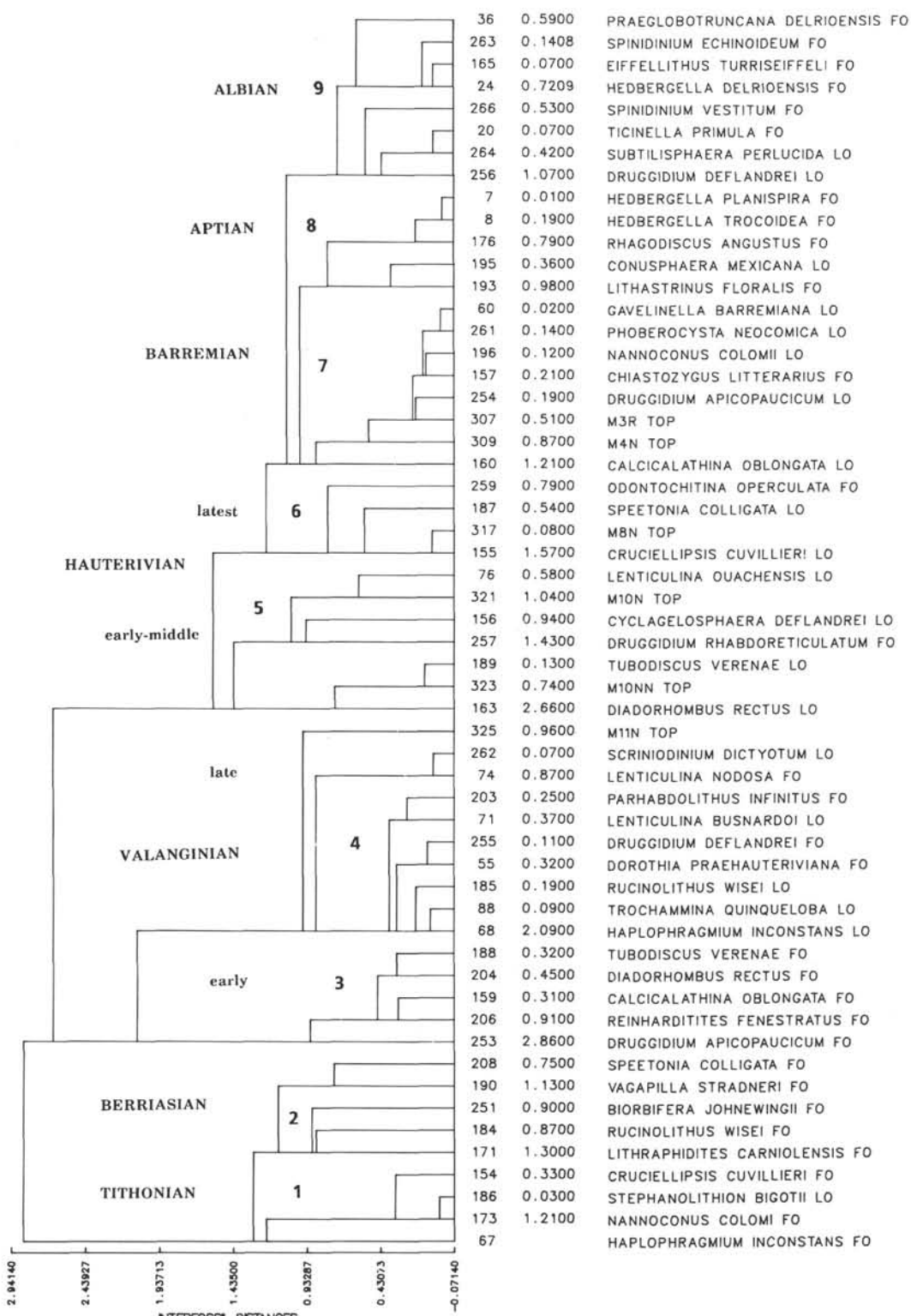


Figure 7. Dendrogram of the FCSS in Figure 6 (right) for 56 latest Jurassic through Early Cretaceous microfossil and magnetic polarity events in 13 DSDP and ODP sites, Atlantic and Indian oceans. The stratigraphic positions are averages of all local relative positions encountered. Nine successive assemblage zones may be differentiated, of Tithonian through Albian age, that form the basis for correlation of the sites in Table 5.

Table 5. Most likely correlation of Late Jurassic and Early Cretaceous zonation events in Figure 7 through all Atlantic and Indian Ocean sites.

Code	Events	DSDP 534A		DSDP 391C		DSDP 603B		DSDP 105		DSDP 370		DSDP 535A		DSDP 416A	
		A	B	A	B	A	B	A	B	A	B	A	B	A	B
36	<i>Praeglobotruncana delrioensis</i> FO (PF)	763.30	774	—	—	—	—	—	—	731.70	740.00	—	—	—	—
263	<i>Spinidinium echinoidaeum</i> FO (P)	793.03	793	—	—	1169.61	1170	335.23	309.00	752.72	—	—	—	—	—
165	<i>Eiffellithus turrieseiffeli</i> FO (N)	800.33	—	—	—	1172.25	—	339.54	322.00	757.96	733.00	—	—	—	—
24	<i>Hedbergella delrioensis</i> FO (PF)	803.92	774	—	—	1173.52	—	341.61	—	760.56	—	—	—	732.98	730.00
266	<i>Spinidinium vestitum</i> FO (P)	843.91	863	811.50	784	1187.10	1188	363.04	388.00	788.89	—	—	—	753.44	—
20	<i>Ticinella primula</i> FO (PF)	872.18	—	852.20	—	1197.19	—	377.25	—	806.45	816.00	327.90	326.00	768.39	—
264	<i>Subiliisphaera perlucida</i> LO (P)	875.58	863	857.11	—	1198.46	—	378.91	392.00	808.22	827.00	330.63	—	770.25	—
256	<i>Druggidium deflandrei</i> LO (P)	896.46	908	886.53	926	1206.75	1210	388.80	404.00	816.96	—	347.93	—	782.16	—
7	<i>Hedbergella planispira</i> FO (PF)	937.05	941	940.86	—	1228.88	1220	407.94	—	827.01	828.00	384.34	368.00	811.10	855.00
8	<i>Hedbergella trocoidea</i> FO (PF)	937.25	—	941.14	927	1229.04	—	408.04	—	827.06	816.00	384.53	404.00	811.28	—
176	<i>Rhagodiscus angustus</i> FO (N)	942.75	—	948.79	963	1233.54	—	410.78	—	828.43	829.00	389.34	—	816.47	764.00
195	<i>Conusphaera mexicana</i> LO (N)	958.99	965	974.38	963	1252.85	1255	419.70	—	835.20	—	402.34	403.00	837.12	—
193	<i>Lithastrinus floralis</i> FO (N)	963.81	—	984.50	—	1262.22	—	422.84	—	839.37	829.00	405.69	—	846.45	—
60	<i>Gavelinella barremiana</i> LO (BF)	972.77	—	1007.63	1009	1287.63	—	428.72	—	852.68	876.00	411.41	—	869.67	—
261	<i>Phoberocysta neocomica</i> LO (P)	972.98	968	1008.13	—	1288.25	1238	428.83	—	852.98	—	411.56	402.00	870.19	—
196	<i>Nannoceras colomii</i> LO (N)	974.25	—	1010.92	1010	1291.78	—	429.40	—	854.62	840.00	412.42	—	873.16	—
157	<i>Chiastozygus littorarius</i> FO (N)	975.38	—	1013.23	1019	1294.71	1324	429.85	—	855.97	—	413.14	422.00	875.62	897.00
254	<i>Druggidium apicopaucicum</i> LO (P)	977.63	—	1017.27	1012	1299.71	1347	430.59	426.00	858.35	—	414.21	—	879.95	—
307	M3r top (M)	979.85	—	1020.71	—	1303.71	—	431.17	—	860.36	—	414.93	—	883.63	—
309	M4n top (M)	987.20	983	1029.52	—	1313.18	1292	432.39	—	865.44	—	416.24	—	892.97	—
160	<i>Calcicalathina oblongata</i> LO (N)	1005.39	991	1043.34	1030	1328.18	1320	433.54	—	873.10	—	418.66	—	907.25	—
259	<i>Odontochitina operculata</i> FO (P)	1036.12	1074	1057.51	1091	1347.95	1373	433.94	433.00	882.37	885.00	430.72	421.00	925.10	—
187	<i>Speetonia colligata</i> LO (N)	1050.53	1018	1058.83	—	1359.54	1330	433.96	—	888.57	—	448.81	459.00	936.80	—
317	M8n top (M)	1061.71	1073	1059.82	—	1368.90	1381	434.04	—	894.08	—	448.59	—	945.30	—
155	<i>Cruciellipsis cuvillieri</i> LO (N)	1063.42	1057	1060.21	1031	1370.34	1360	434.06	430.00	895.01	891.00	448.81	444.00	946.57	982.00
76	<i>Lenticulina ouachensis</i> LO (BF)	1097.50	—	1083.28	—	1400.02	—	435.29	—	922.10	—	450.15	—	980.18	900.00
321	M10n top (M)	1106.99	1112	1095.71	—	1408.86	1423	436.10	—	935.41	—	451.69	—	999.41	—
156	<i>Cyclagelosphaera deflandrei</i> LO (N)	1115.52	1130	1116.67	1126	1418.89	1427	438.03	—	962.43	—	460.78	—	1042.29	—
257	<i>Druggidium rhabdoreticulatum</i> FO (P)	1116.58	1099	1129.49	1131	1424.89	1404	440.29	440.00	989.18	—	480.40	478.00	1085.86	—
189	<i>Tubodiscus verenae</i> LO (N)	1127.51	1127	1139.24	1137	1438.31	1446	444.58	—	1030.93	—	533.98	531.00	1149.50	1188.00
323	M10Nn top (M)	1129.14	1128	1139.84	—	1439.66	1447	445.04	—	1034.87	—	539.94	—	1154.92	—
163	<i>Diadorhombus rectus</i> LO (N)	1138.62	1143	1142.69	—	1446.95	1436	447.67	—	1055.60	—	570.29	576.00	1181.55	1199.00
325	M11n top (M)	1169.20	1172	1153.38	—	1479.82	1493	458.73	—	1114.29	—	614.22	—	1250.97	—
262	<i>Scriniodinium dictyonum</i> LO (P)	1179.16	1193	1160.36	—	1492.14	1476	463.24	459.00	1125.71	—	620.90	—	1274.56	—
74	<i>Lenticulina nodosa</i> FO (BF)	1179.84	1167	1160.91	1147	1493.02	—	463.54	469.00	1126.20	1129.00	621.45	—	1276.16	1303.00
203	<i>Parhabdolithus infinitus</i> FO (N)	1191.85	1189	1168.69	1198	1507.28	—	467.78	—	1130.18	—	632.88	611.00	1301.66	—
71	<i>Lenticulina busnardoii</i> LO (BF)	1196.42	—	1170.32	—	1511.80	1509	469.05	—	1130.48	1139.00	637.52	660.00	1310.44	1222.00
255	<i>Druggidium deflandrei</i> FO (P)	1204.06	1205	1172.37	1177	1518.41	1518	470.91	484.00	1130.53	—	642.57	—	1324.55	—
55	<i>Dorothia prehauteriviana</i> FO (BF)	1206.63	1167	1173.03	1147	1520.41	1509	471.48	457.00	1130.56	1120.00	643.67	—	1329.16	1400.00
185	<i>Rucinolithus wieseii</i> LO (N)	1214.44	1223	1175.23	1178	1525.97	1546	473.17	—	1130.89	—	645.89	—	1343.11	1391.00
88	<i>Trochammina quinqueloba</i> LO (BF)	1218.80	1149	1176.69	—	1528.97	—	474.17	—	1131.26	—	646.65	—	1351.81	1198.00
68	<i>Haplophragmium inconstans</i> LO (BF)	1220.71	1332	1177.42	—	1530.33	—	474.66	—	1131.49	—	646.91	—	1356.12	—
188	<i>Tubodiscus verenae</i> FO (N)	1231.98	1230	1198.20	1198	1548.54	1556	487.07	—	1144.77	1140.00	652.98	648.00	1468.03	1531.00
204	<i>Diadorhombus rectus</i> FO (N)	1233.36	1207	1201.31	1199	1549.02	1565	489.11	—	1148.05	—	657.39	—	1483.07	—
159	<i>Calcicalathina oblongata</i> FO (N)	1237.21	1230	1205.28	1210	1549.13	1526	492.03	—	1152.71	1158.00	665.17	—	1501.96	1531.00
206	<i>Reinhardtites fenestratus</i> FO (N)	1240.44	1269	1207.60	1210	1549.34	—	494.12	—	1155.69	—	670.84	675.00	1513.52	—
253	<i>Druggidium apicopaucicum</i> FO (P)	1247.54	1243	1212.27	1212	1551.38	1549	500.20	504.00	1162.68	—	684.98	684.00	1539.32	—
208	<i>Speetonia colligata</i> FO (N)	1273.25	1272	1224.99	—	1566.75	1570	522.18	—	1174.55	—	—	—	1570.62	—
190	<i>Vagapilla stradneri</i> FO (N)	1283.51	1288	1232.44	1229	1570.40	—	529.49	—	1176.39	1176.00	—	—	1571.56	—
251	<i>Biorbifera johnnewigii</i> FO (P)	1303.59	1287	1249.85	1263	1575.11	1574	542.49	533.00	—	—	—	—	1571.77	—
184	<i>Rucinolithus wieseii</i> FO (N)	1325.03	1331	1270.11	1238	—	—	554.85	—	—	—	—	—	1573.18	1560.00
171	<i>Lithraphidites carniolensis</i> FO (N)	1341.87	1353	1298.13	1312	—	—	567.90	—	—	—	—	—	1577.32	1559.00
154	<i>Cruciellipsis cuvillieri</i> FO (N)	1351.04	1359	1338.76	1372	—	—	588.30	603.00	—	—	—	—	1588.74	1615.00
186	<i>Stephanolithion bigotii</i> LO (N)	1351.30	1350	1347.17	—	—	—	593.44	585.00	—	—	—	—	1592.19	—
173	<i>Nannoconus colomi</i> FO (N)	1351.31	1340	1347.99	1321	—	—	—	—	—	—	—	—	1592.55	1572.00
67	<i>Haplophragmium inconstans</i> FO (BF)	1351.90	1352	—	—	—	—	—	—	—	—	—	—	1606.57	1616.00

To the extreme left is the FCSS; Column B contains the measured depth per site of the actually observed record; the interpolated (average) depth for the events in the FCSS is in Column A. Dashes in both columns indicate absence of data for executing spline crossplots between zonation and individual site record.

Table 5 (continued).

Code	Events	DSDP 398d		DSDP 367		DSDP 387		ODP 765		DSDP 261		ODP 766	
		A	B	A	B	A	B	A	B	A	B	A	B
36	<i>Praeglobotruncana delrioensis</i> FO (PF)	—	—	698.80	701.00	—	—	—	—	—	—	—	—
263	<i>Spinidinium echinoideum</i> FO (P)	—	—	711.46	—	—	—	—	—	—	—	—	—
165	<i>Eiffellithus turrisifeli</i> FO (N)	994.37	993.00	714.43	727.00	474.49	469.00	—	—	—	—	—	—
24	<i>Hedbergella delrioensis</i> FO (PF)	1009.36	—	715.86	730.00	477.85	—	729.51	721.00	—	—	—	—
266	<i>Spinidinium vestitum</i> FO (P)	1160.45	—	731.46	—	513.01	—	738.26	—	—	—	—	—
20	<i>Ticinella primula</i> FO (PF)	1245.67	1250.00	743.82	730.00	536.89	—	744.69	—	—	—	—	—
264	<i>Subtilisphaera perlucida</i> LO (P)	1253.89	—	745.45	—	539.69	—	745.50	—	—	—	—	—
256	<i>Druggidium deflandrei</i> LO (P)	1296.21	—	756.49	—	556.39	565.00	750.68	—	—	—	—	—
7	<i>Hedbergella planispira</i> FO (PF)	1419.97	1345.00	788.83	787.00	587.21	—	763.58	712.00	—	—	—	—
8	<i>Hedbergella trocoidea</i> FO (PF)	1421.31	1468.00	789.07	701.00	587.37	—	763.66	—	—	—	—	—
176	<i>Rhagodiscus angustus</i> FO (N)	1460.02	1487.00	795.91	—	591.62	—	766.04	726.00	—	—	—	—
195	<i>Conusphaera mexicana</i> LO (N)	1554.58	—	824.94	—	605.54	603.00	775.52	—	—	—	—	—
193	<i>Lithastrinus floralis</i> FO (N)	1572.06	1571.00	838.41	891.00	610.70	—	779.89	—	—	—	—	—
60	<i>Gavelinella barremiana</i> LO (BF)	1585.09	1591.00	870.99	—	621.31	—	791.33	—	—	—	—	—
261	<i>Phoberocystis neocomica</i> LO (P)	1585.09	—	871.71	—	621.52	—	791.61	863.00	—	—	—	—
196	<i>Nannoconus colomii</i> LO (N)	1585.33	1573.00	875.73	897.00	622.65	—	793.18	—	—	—	—	—
157	<i>Chiastozygus litterarius</i> FO (N)	1586.28	1592.00	879.04	891.00	623.56	—	794.50	724.00	—	—	—	—
254	<i>Druggidium apicopaucicum</i> LO (P)	1588.83	—	884.80	—	625.08	—	796.91	—	—	—	—	—
307	M3r top (M)	1591.70	—	889.63	—	626.29	—	799.02	833.00	417.96	404.00	276.15	259.00
309	M4n top (M)	1602.01	—	901.45	—	628.97	—	804.66	845.00	422.44	438.00	284.82	—
160	<i>Calcicalathina oblongata</i> LO (N)	1625.93	1626.00	917.81	916.00	631.76	632.00	813.97	—	429.73	—	299.66	—
259	<i>Odontochitina operculata</i> FO (P)	1665.48	—	933.67	—	632.96	633.00	826.04	816.00	439.05	—	320.02	—
187	<i>Speetonia colligata</i> LO (N)	1693.53	—	940.67	—	633.01	—	833.39	—	444.80	—	333.17	—
317	M8s top (M)	1713.16	—	944.27	—	633.10	—	838.15	—	448.64	—	342.05	346.00
155	<i>Cruciellipsis cuvillieri</i> LO (N)	1715.98	1716.00	944.72	940.00	633.14	633.00	838.81	873.00	449.18	447.00	343.31	272.00
76	<i>Lenticulina ouachensis</i> LO (BF)	—	—	950.93	—	635.92	—	851.19	882.00	459.91	—	368.10	422.00
321	M10n top (M)	—	—	952.09	—	638.48	—	855.27	—	463.73	—	376.70	400.00
156	<i>Cyclagelosphaera deflandrei</i> LO (N)	—	—	953.15	—	646.16	642.00	861.99	—	470.33	—	391.20	—
257	<i>Druggidium rhabdotreticulatum</i> FO (P)	—	—	953.39	—	656.54	660.00	867.42	—	475.96	—	403.23	—
189	<i>Tubodiscus verenae</i> LO (N)	—	—	953.53	—	672.91	—	874.57	866.00	483.78	—	419.39	443.00
323	M10Nn top (M)	—	—	953.58	—	674.45	—	875.19	—	484.48	—	420.80	425.00
163	<i>Diadorhombus rectus</i> LO (N)	—	—	954.09	—	682.71	—	878.37	—	488.07	—	428.04	—
325	M11n top (M)	—	—	962.19	—	711.56	—	887.47	—	489.23	—	448.98	441.00
262	<i>Scriniodinium dictyonum</i> LO (P)	—	—	969.00	—	721.87	—	889.99	—	500.71	—	454.92	—
74	<i>Lenticulina nodosa</i> FO (BF)	—	—	969.52	—	722.52	—	890.14	—	500.84	—	455.27	—
203	<i>Parhabdolithus infinitus</i> FO (N)	—	—	978.28	941.00	731.79	—	892.08	—	502.40	—	459.92	—
71	<i>Lenticulina busnardoi</i> LO (BF)	—	—	981.31	—	734.47	—	892.59	—	502.73	—	461.15	—
255	<i>Druggidium deflandrei</i> FO (P)	—	—	985.94	—	738.35	735.00	893.28	—	503.11	—	462.85	—
55	<i>Dorothia praehaueriviana</i> FO (BF)	—	—	987.39	—	739.53	—	893.49	893.00	503.20	—	463.35	—
185	<i>Rucinolithus wisei</i> LO (N)	—	—	991.57	1024.00	742.85	746.00	894.05	883.00	503.40	—	464.73	—
88	<i>Trochammina quinqueloba</i> LO (BF)	—	—	994.00	—	774.70	—	894.36	908.00	503.47	525.00	465.50	—
68	<i>Haplophragmium inconstans</i> LO (BF)	—	—	995.14	—	745.56	—	894.51	891.00	503.50	494.00	465.86	—
188	<i>Tubodiscus verenae</i> FO (N)	—	—	1020.31	—	760.07	773.00	897.26	892.00	504.29	487.00	472.81	471.00
204	<i>Diadorhombus rectus</i> FO (N)	—	—	1023.86	1024.00	761.38	746.00	897.58	—	504.84	—	473.65	—
159	<i>Calcicalathina oblongata</i> FO (N)	—	—	1028.73	—	763.60	765.00	897.99	—	505.90	—	474.74	—
206	<i>Reinhardtiites fenestratus</i> FO (N)	—	—	1032.04	—	765.38	—	898.26	—	506.82	506.00	475.44	—
253	<i>Druggidium apicopaucicum</i> FO (P)	—	—	1041.03	—	770.82	772.00	898.91	—	510.00	—	477.18	—
208	<i>Speetonia colligata</i> FO (N)	—	—	1064.77	—	784.87	—	900.08	—	520.40	532.00	480.54	—
190	<i>Vagapilla stradneri</i> FO (N)	—	—	1069.71	—	787.43	788.00	900.22	—	521.81	—	480.98	—
251	<i>Biorbifera johnewingii</i> FO (P)	—	—	1076.10	—	790.53	790.00	900.34	—	522.79	—	481.41	—
184	<i>Rucinolithus wisei</i> FO (N)	—	—	1180.29	1083.00	—	—	900.39	893.00	523.04	—	481.59	—
171	<i>Lithraphidites carniolensis</i> FO (N)	—	—	1083.55	1085.00	—	—	900.42	—	523.23	—	481.68	—
154	<i>Cruciellipsis cuvillieri</i> FO (N)	—	—	1087.46	1087.00	—	—	900.43	893.00	524.20	507.00	481.70	471.00
186	<i>Stephanolithion bigottii</i> LO (N)	—	—	1088.36	—	—	—	—	—	524.69	532.00	—	—
173	<i>Nannoconus colomi</i> FO (N)	—	—	1088.45	1085.00	—	—	—	—	524.74	—	—	—
67	<i>Haplophragmium inconstans</i> FO (BF)	—	—	—	—	—	—	—	—	527.04	532.00	—	—

graphic methods, STRATCOR and RASC, provide powerful and efficient tools for solving this problem. STRATCOR also is suited for smaller data sets, such as those encountered here.

The STRATCOR-derived Final Composite Standard Sequence (FCSS) displays the most likely, average order of 56 stratigraphic events based on geomagnetic reversals and the average range endpoints of nannofossils, planktonic and benthic foraminifers, and dinocysts. Each event occurs in at least three sites. Nine assemblage zones of Tithonian through Albian age are proposed; the zonation may be refined using more data, although for optimum resolution, it is best to erect separate Atlantic and Indian Ocean zonations. Using STRATCOR, the FCSS also is correlated through all ocean sites.

ACKNOWLEDGMENTS

This study and its manuscript benefitted from scientific advice provided by Inger Lise Kristiansen, Mike Kaminski, Jurgen Muttemlose, and Sherwood Wise. Doug Williams, Frits Agterberg, and Jill Mutschler-Fontenot suggested improvements of the manuscript. We are grateful for the support provided by these colleagues. Art Jackson and Frank Thomas, Dartmouth, Nova Scotia, gave valuable technical assistance. The authors acknowledge financial support for this study from the Geological Survey of Canada (to FMG and DM), the National Science and Engineering Research Council (NSERC) (to ZH), and the National Science Foundation (to JGO).

REFERENCES

- Agterberg, F. P., 1990. *Automated Stratigraphic Correlation*: New York (Elsevier).
- Agterberg, F. P., Gradstein, F. M., Nel, L. D., Lew, S. N., Heller, M., Gradstein, W. S., D'Iorio, M. D., Gillis, D., and Huang, Z., 1989. Program RASC (ranking and scaling). *Com. Quant. Stratigr. IUGS*, Version 12 (manual and diskette).
- Blechschmidt, C., 1979. Biostratigraphy of calcareous nannofossils: Leg 47B, Deep Sea Drilling Project. In Sibuet, J., Ryan, W.B.F., et al., *Init. Repts. DSDP*, 47(Pt. 2): Washington (U.S. Govt. Printing Office), 327–360.
- Ceppek, P., 1978. Mesozoic calcareous nannoplankton of the eastern North Atlantic, Leg 41. In Lancelot, Y., Seibold, E., et al., *Init. Repts. DSDP*, 41: Washington (U.S. Govt. Printing Office), 667–688.
- Cepkek, P., Gartner, S., and Cool, T., 1980. Mesozoic calcareous nannofossils, Deep Sea Drilling Project Sites 415 and 416, Moroccan Basin. In Lancelot, Y., Winterer, E. L., et al., *Init. Repts. DSDP*, 50: Washington (U.S. Govt. Printing Office), 345–354.
- Covington, J. M., and Wise, S. W., Jr., 1987. Calcareous nannofossil biostratigraphy of a Lower Cretaceous deep-sea fan complex, Deep Sea Drilling Project Leg 93, Site 603, lower continental rise off Cape Hatteras. In van Hinte, J. E., Wise, S. W., Jr., et al., *Init. Repts. DSDP*, 93 (Pt. 2): Washington (U.S. Govt. Printing Office), 617–660.
- Edwards, L. E., 1984. Insight on why graphic correlation (Shaw's method) works. *J. Geol.*, 92:583–597.
- Gradstein, F. M., 1978a. Foraminifera from DSDP Site 370, Leg 41, eastern North Atlantic Ocean. In Talwani, M., Udrinsev, G., et al., *Init. Repts. DSDP*, 38–41 (Supplement to Vols. XXXVIII, XXXIX, XL, and XLI): Washington (U.S. Govt. Printing Office), 779–782.
- , 1978b. Biostratigraphy of Lower Cretaceous Blake Nose and Blake-Bahama Basin foraminifers, DSDP Leg 44, western North Atlantic Ocean. In Benson, W. E., Sheridan, R. E., et al., *Init. Repts. DSDP*, 44: Washington (U.S. Govt. Printing Office), 663–702.
- , 1983. Paleoecology and stratigraphy of Jurassic abyssal foraminifera in the Blake-Bahama Basin, Deep Sea Drilling Project Leg 76, Sites 533 and 534. In Gradstein, F. M., Sheridan, R. E., et al., *Init. Repts. DSDP*, 76: Washington (U.S. Govt. Printing Office), 537–560.
- , 1986. Northwestern Atlantic Mesozoic biostratigraphy. In Vogt, P. R., and Tucholke, B. (Eds.), *The Geology of North America*, Vol. M, *The Western North Atlantic Region*: Alexandria, VA (Geol. Soc. Am.), 507–525.
- , 1990. Program STRATCOR (Version 1.6) for zonation and correlation of fossil events. *Geol. Surv. Can. Rept.*, 2285 (incl. manual + program diskette).
- Gradstein, F. M., and Agterberg, F. P., 1982. Models of Cenozoic foraminiferal stratigraphy, northwestern Atlantic margin. In Cubitt, J. M., and Reament, R. A. (Eds.), *Quantitative Stratigraphic Correlation*: Chichester (Wiley), 265–270.
- Gradstein, F. M., Agterberg, F. P., Brower, J. C., Schwarzacher, W., 1985. *Quantitative Stratigraphy*: New York (Reidel and Unesco Publ. Co.).
- Habib, D., 1972. Dinoflagellate stratigraphy, Leg XI, Deep Sea Drilling Project. In Hollister, C. D., Ewing, J. I., et al., *Init. Repts. DSDP*, 11: Washington (U.S. Govt. Printing Office), 367–426.
- , 1977. Comparison of Lower and Middle Cretaceous palynostratigraphic zonations in the western North Atlantic. In Swain, F. M. (Ed.), *Stratigraphic Micropaleontology of Atlantic Basin and Borderlands*: New York (Elsevier), 341–368.
- , 1979. Palynostratigraphy of Cretaceous sediments from Site 387, western Bermuda Rise. In Tucholke, B. E., and Vogt, P. R., et al., *Init. Repts. DSDP*, 43: Washington (U.S. Govt. Printing Office), 585–590.
- , 1978. Palynostratigraphy of the Lower Cretaceous section at DSDP Site 391, Blake-Bahama Basin, and its correlation in the North Atlantic. In Benson, W. E., Sheridan, R. E., et al., *Init. Repts. DSDP*, 44: Washington (U.S. Govt. Printing Office), 887–898.
- Habib, D., and Knapp, S., 1982. Stratigraphic utility of Cretaceous small acritarchs. *Micropaleontology*, 28:335–371.
- Habib, D., and Drugg, W. S., 1983. Dinoflagellate age of Middle Jurassic-Early Cretaceous sediments in the Blake-Bahama Basin. In Gradstein, F. M., Sheridan, R. E., et al., *Init. Repts. DSDP*, 76: Washington (U.S. Govt. Printing Office), 623–638.
- , 1987. Palynology of Sites 603 and 605, Leg 93, Deep Sea Drilling Project. In van Hinte, J. E., Wise, S. W., Jr., et al., *Init. Repts. DSDP*, 93(Pt. 2): Washington (U.S. Govt. Printing Office), 751–776.
- Harland, W. B., Armstrong, R. L., Cox, A. V., Craig, L. E., Smith, A. G., and Smith, D. G., 1990. *A Geological Time Scale*: Cambridge (Cambridge Univ. Press).
- Jansa, L. F., Enos, P., Tucholke, B. E., Gradstein, F. M., and Sheridan, R. E., 1979. Mesozoic-Cenozoic sedimentary formations of the North American Basin; western North Atlantic. In Talwani, M., Hay, W., and Ryan, W.B.F., (Eds.), *Deep Drilling Results in the Atlantic Ocean: Continental Margins and Paleoenvironment* Washington (Am. Geophys. Union), Maurice Ewing Ser., 3:1–57.
- Kent, D. V., and Gradstein, F. M., 1985. A Jurassic and Cretaceous geochronology. *Geol. Soc. Am. Bull.*, 96:1419–1427.
- Kuznetsova, K. I., and Seibold, I., 1978. Foraminifers from the Upper Jurassic and Lower Cretaceous of the eastern Atlantic (DSDP Leg 41, Sites 367 and 370). In Lancelot, Y., Seibold, E., et al., *Init. Repts. DSDP*, 41: Washington (U.S. Govt. Printing Office), 515–538.
- Leckie, R. M., 1984. Mid-Cretaceous planktonic foraminiferal biostratigraphy off central Morocco, Deep Sea Drilling Project Leg 79, Sites 545 and 547. In Hinz, K., Winterer, E. L., et al., *Init. Repts. DSDP*, 79: Washington (U.S. Govt. Printing Office), 579–620.
- Lowrie, W., and Ogg, J. G., 1985. A magnetic polarity time scale for Early Cretaceous and Late Jurassic. *Earth Planet. Sci. Lett.*, 76:341–349.
- Ludden, J. N., and Gradstein, F. M., et al., 1990. *Proc. ODP Init. Repts.*, 123: College Station, TX (Ocean Drilling Program).
- Luterbacher, H., 1972. Foraminifera from the Lower Cretaceous and Upper Jurassic of the northwestern Atlantic. In Hollister, C. D., Ewing, J. I., et al., *Init. Repts. DSDP*, 11: Washington (U.S. Govt. Printing Office), 561–594.
- McNulty, C. L., 1979. Smaller Cretaceous foraminifers of Leg 43, Deep Sea Drilling Project. In Tucholke, B. E., and Vogt, P. R., et al., *Init. Repts. DSDP*, 43: Washington (U.S. Govt. Printing Office), 487–506.
- Miller, F. X., 1977. The graphic correlation method in biostratigraphy. In Kauffman, E. G., and Hazel, J. E. (Eds.), *Concepts and Methods of Biostratigraphy*: Stroudsburg, PA (Hutchinson and Ross), 165–186.
- Ogg, J. G., 1983. Magnetostratigraphy of Upper Jurassic and Lowermost Cretaceous sediments, Deep Sea Drilling Project Site 534, western North Atlantic. In Gradstein, F. M., Sheridan, R. E., et al., *Init. Repts. DSDP*, 76: Washington (U.S. Govt. Printing Office), 685–698.
- , 1987. Early Cretaceous magnetic polarity time scale and the magnetostratigraphy of Deep Sea Drilling Project Sites 603 and 534, western central Atlantic. In van Hinte, J. E., Wise, S. W., Jr., et al., *Init. Repts. DSDP*, 93 (Pt. 2): Washington (U.S. Govt. Printing Office), 849–880.
- , in press. Jurassic magnetic polarity time scale. In Westermann, G.E.G. (Ed.), *Circum-Pacific Jurassic*: New York (Elsevier).

- Ogg, J. G., and Steiner, M. B., 1988. Late Jurassic and Early Cretaceous magnetic polarity time scale. In Rocha, R. (Ed.), *Proc. 2nd Int. Symp. Jurassic Stratigr.* (Lisbon, Sept. 1987), 1125–1138.
- Okada, H., and Thierstein, H. R., 1979. Calcareous nannoplankton—Leg 43, Deep Sea Drilling Project. In Tucholke, B. E., and Vogt, P. R., et al., *Init. Repts. DSDP*, 43: Washington (U.S. Govt. Printing Office), 507–574.
- Pflaumann, U., and Krasheninnikov, V. A., 1978. Early Cretaceous planktonic foraminifers from eastern North Atlantic, DSDP Leg 41. In Lancelot, Y., Seibold, E., et al., *Init. Repts. DSDP*, 41: Washington (U.S. Govt. Printing Office), 539–564.
- Riley, L. A., and Fenton, J.P.G., 1984. Palynostratigraphy of the Berriasian to Cenomanian sequence at Deep Sea Drilling Project Site 535, Leg 77, southeastern Gulf of Mexico. In Buffler, R. T., Schlager, W., et al., *Init. Repts. DSDP*, 77: Washington (U.S. Govt. Printing Office), 675–690.
- Roth, P. R., 1983. Jurassic and Lower Cretaceous calcareous nannofossils in the western North Atlantic (Site 534): biostratigraphy, preservation, and some observations on biogeography and paleoceanography. In Gradstein, F. M., Sheridan, R. E., et al., *Init. Repts. DSDP*, 76: Washington (U.S. Govt. Printing Office), 587–622.
- Roth, P. R., 1978. Cretaceous nannoplankton biostratigraphy and oceanography of the northwestern Atlantic Ocean. In Benson, W. E., Sheridan, R. E., et al., *Init. Repts. DSDP*, 44: Washington (U.S. Govt. Printing Office), 731–760.
- Schmidt, R. R., 1978. Calcareous nannoplankton from the western North Atlantic, DSDP Leg 44. In Benson, W. E., Sheridan, R. E., et al., *Init. Repts. DSDP*, 44: Washington (U.S. Govt. Printing Office), 703–730.
- Shaw, A. B., 1964. *Time in Stratigraphy*: New York (McGraw-Hill).
- Sigal, J., 1979. Chronostratigraphy and ecostratigraphy of Cretaceous formations recovered on DSDP Leg 47B, Site 398. In Sibuet, J., Ryan, W.B.F., et al., *Init. Repts. DSDP*, 47 (Pt. 2): Washington (U.S. Govt. Printing Office), 287–326.
- Silva, I. P., and McNulty, C. L. 1984. Planktonic foraminifers and calpionellids from Gulf of Mexico sites, Deep Sea Drilling Project Leg 77. In Buffler, R. T., Schlager, W., et al., *Init. Repts. DSDP*, 77: Washington (U.S. Govt. Printing Office), 547–584.
- Sliter, W. V., 1980. Mesozoic foraminifers and deep-sea benthic environments from Deep Sea Drilling Project Sites 415 and 416, eastern North Atlantic. In Lancelot, Y., Winterer, E. L., et al., *Init. Repts. DSDP*, 50: Washington (U.S. Govt. Printing Office), 353–428.
- Sliter, W. V., and Silva, I. P., 1984. Autochthonous and displaced (allochthonous) Cretaceous benthic foraminifers from Deep Sea Drilling Project Leg 77, Sites 535, 536, 537, 538 and 540, Gulf of Mexico. In Buffler, R. T., Schlager, W., et al., *Init. Repts. DSDP*, 77: Washington (U.S. Govt. Printing Office), 593–629.
- Watkins, D. K., and Bowdler, J. L., 1984. Cretaceous nannofossils from Deep Sea Drilling Project Leg 77, southeast Gulf of Mexico. In Buffler, R. T., Schlager, W., et al., *Init. Repts. DSDP*, 77: Washington (U.S. Govt. Printing Office), 649–674.
- Wiegand, G. E., 1984. Cretaceous nannofossils from the northwest African margin, Deep Sea Drilling Project Leg 79. In Hinz, K., Winterer, E. L., et al., *Init. Repts. DSDP*, 79: Washington (U.S. Govt. Printing Office), 563–579.
- Wilcoxon, J. A., 1972. Calcareous nannoplankton ranges, Leg 11, Deep Sea Drilling Project. In Hollister, C. D., Ewing, J. I., et al., *Init. Repts. DSDP*, 11: Washington (U.S. Govt. Printing Office), 459–474.
- Williams, G. L., 1978. Palynological biostratigraphy, Deep Sea Drilling Project Sites 367 and 370. In Talwani, M., Udintsev, G., et al., *Init. Repts. DSDP*, 38–41 (Supp. Vol. 38, 39, 40, and 41): Washington (U.S. Govt. Printing Office), 779–782.

123B-116

Date of initial receipt: 18 January 1991

Date of acceptance: 2 April 1991

APPENDIX A
Numerical Dictionary for Stratigraphic Events in 13 DSDP and ODP Sites

Number	Name	Number	Name
1	<i>Caucasella huterivica</i> FO (PF)	193	<i>Lithastrinus floralis</i> FO (N)
2	<i>Caucasella huterivica</i> LO (PF)	194	<i>Vagapilla matalosa</i> FO (N)
7	<i>Hedbergella planispira</i> FO (PF)	195	<i>Conusphaera mexicana</i> LO (N)
8	<i>Hedbergella trocoidea</i> FO (PF)	196	<i>Nannoconus colomii</i> LO (N)
10	<i>Planomalina buxtorfi</i> LO (PF)	197	<i>Nannoconus truitti</i> FO (N)
12	<i>Rotalipora appenninica</i> FO (PF)	200	<i>Chiastozygus striatus</i> FO (N)
13	<i>Rotalipora appenninica</i> LO (PF)	202	<i>Nannoconus bucheri</i> FO (N)
18	<i>Ticinella breggiensis</i> FO (PF)	203	<i>Parhabdolithus infinitus</i> FO (N)
19	<i>Ticinella breggiensis</i> LO (PF)	204	<i>Diadorhombus rectus</i> FO (N)
20	<i>Ticinella primula</i> FO (PF)	206	<i>Reinhardittes fenestratus</i> FO (N)
21	<i>Ticinella roberti</i> FO (PF)	208	<i>Speetonia colligata</i> FO (N)
22	<i>Ticinella roberti</i> LO (PF)	209	<i>Prediscosphaera cretacea</i> FO (N)
24	<i>Hedbergella delrioensis</i> FO (PF)	210	<i>Cyclagelosphaera deflandrei</i> (N) FO
26	<i>Globigerinelloides blowi</i> FO (PF)	211	<i>Crucibiscutum salebrosum</i> (N) FO
27	<i>Globigerinelloides blowi</i> LO (PF)	212	<i>Tegumentum striatum</i> (N) FO
29	<i>Globigerinelloides ferreolensis</i> LO (PF)	213	<i>Tegumentum striatum</i> (N) LO
32	<i>Hedbergella simplex</i> FO (PF)	214	<i>Tegumentum triples</i> (N) FO
36	<i>Praeglobotruncana delrioensis</i> FO (PF)	215	<i>Tegumentum triples</i> (N) LO
37	<i>Praeglobotruncana delrioensis</i> LO (PF)	216	<i>Eprolithus apertior</i> (N) FO
40	<i>Hedbergella sigali</i> FO (PF)	217	<i>Eprolithus varoli</i> (N) FO
41	<i>Hedbergella sigali</i> LO (PF)	218	<i>Flabellites biforaminis</i> (N) FO
55	<i>Dorothia praehauteriviana</i> FO (BF)	219	<i>Corolithion achylosus</i> (N) FO
56	<i>Epistomina uhligi</i> LO (BF)	220	<i>Hayesites irregularis</i> (N) FO
57	<i>Epistomina caracolla</i> LO (BF)	221	<i>Prediscosphaera columnata</i> (N) FO
60	<i>Gavelinella barremiana</i> LO (BF)	251	<i>Biorbisera johnnewingii</i> FO (P)
67	<i>Haplophragmium inconstans</i> FO (BF)	253	<i>Druggidium apicopaucicum</i> FO (P)
68	<i>Haplophragmium inconstans</i> LO (BF)	254	<i>Druggidium apicopaucicum</i> LO (P)
70	<i>Lenticulina busnardoii</i> FO (BF)	255	<i>Druggidium deflandrei</i> FO (P)
71	<i>Lenticulina busnardoii</i> LO (BF)	256	<i>Druggidium deflandrei</i> LO (P)
72	<i>Lenticulina crepidularis</i> LO (BF)	257	<i>Druggidium rhabdoreticulatum</i> FO (P)
74	<i>Lenticulina nodosa</i> FO (BF)	259	<i>Odontochitina operculata</i> FO (P)
76	<i>Lenticulina ouachensis</i> LO (BF)	261	<i>Phoberocysta neocomica</i> LO (P)
78	<i>Lenticulina quenstedti</i> LO (BF)	262	<i>Scriniodinium dictyonum</i> LO (P)
87	<i>Trochammina quinqueloba</i> FO (BF)	263	<i>Spinidinium echinoideum</i> FO (P)
88	<i>Trochammina quinqueloba</i> LO (BF)	264	<i>Subtilisphaera perlucida</i> LO (P)
89	<i>Verneuilinoides neocomiensis</i> LO (BF)	266	<i>Spinidinium vestitum</i> FO (P)
90	<i>Verneuilinoides neocomiensis</i> FO (BF)	267	<i>Diconodinium davidii</i> (P) FO
91	<i>Pseudoreopax cisochnicensis</i> FO (BF)	268	<i>Diconodinium davidii</i> (P) LO
92	<i>Paalzowella feifeli</i> LO (BF)	269	<i>Pseudoceratium turneri</i> (P) FO
93	<i>Epistomina caracolla</i> P (BF)	270	<i>Dingodinium cerviculum</i> (P) LO
94	<i>Gavelinella bettenstaedti</i> P (BF)	271	<i>Rhombodella paucispina</i> (P) LO
95	<i>Hormosina cf. crassa</i> FO (BF)	272	<i>Ascodinium</i> sp. A (P) PEAK
96	<i>Dorothia praehauteriviana</i> LO (BF)	273	<i>Muderongia australis</i> (P) FO
97	<i>Gavelinella barremiana</i> FO (BF)	274	<i>Batioladinium reticulatum</i> (P) P
98	<i>Conorboides hofkeri</i> FO (BF)	275	<i>Dissimilidinium ibispinosum</i> (P) LO
100	<i>Lenticulina ouachensis</i> FO (BF)	276	<i>Egmontidinium torynum</i> (P) P
101	<i>Epistomina caracolla</i> FO (BF)	301	M0r top (M)
154	<i>Cruciellipsis cuvilliieri</i> FO (N)	303	M1n top (M)
155	<i>Cruciellipsis cuvilliieri</i> LO (N)	304	M1r top (M)
156	<i>Cyclagelosphaera deflandrei</i> LO (N)	305	M2n top (M)
157	<i>Chiastozygus litterarius</i> FO (N)	307	M3r top (M)
158	<i>Conusphaera mexicana</i> FO (N)	309	M4n top (M)
159	<i>Calcidalathina oblongata</i> FO (N)	311	M5r top (M)
160	<i>Calcidalathina oblongata</i> LO (N)	315	M7n top (M)
163	<i>Diadorhombus rectus</i> LO (N)	316	M7r top (M)
164	<i>Eiffellithus eximus</i> FO (N)	317	M8n top (M)
165	<i>Eiffellithus turrisieffeli</i> FO (N)	318	M8r top (M)
171	<i>Lithraphidites carniolensis</i> FO (N)	319	M9n top (M)
173	<i>Nannoconus colomi</i> FO (N)	321	M10n top (M)
176	<i>Rhagodiscus angustus</i> FO (N)	322	M10r top (M)
180	<i>Rucinolithus irregularis</i> FO (N)	323	M10Nn top (M)
184	<i>Rucinolithus wisei</i> FO (N)	324	M10Nr top (M)
185	<i>Rucinolithus wisei</i> LO (N)	325	M11n top (M)
186	<i>Stephanolithion bigotii</i> LO (N)	338	M15r top (M)
187	<i>Speetonia colligata</i> LO (N)	339	M16n top (M)
188	<i>Tubodiscus verenae</i> FO (N)	340	M16r top (M)
189	<i>Tubodiscus verenae</i> LO (N)		
190	<i>Vagapilla stradneri</i> FO (N)		
191	<i>Tranolithus orionatus</i> FO (N)		

Number of entries printed: 135

APPENDIX B
Listing of all Microfossil and Geomagnetic Polarity Events in 10 Atlantic and 3 Indian Ocean Sites (used here)

1. DSDP Leg 76, Hole 534A, Western Atlantic Ocean.

Depth	Number	Fossil Name
00774.	36	<i>Praeglobotruncana delrioensis</i> FO (PF)
	24	<i>Hedbergella delrioensis</i> FO (PF)
00793.	263	<i>Spinidinium echinoideum</i> FO (P)
00831.	191	<i>Tranolithus orionatus</i> FO (N)
00863.	266	<i>Spinidinium vestitum</i> FO (P)
	264	<i>Subtilisphaera perlucida</i> LO (P)
00908.	256	<i>Druggidium deflandrei</i> LO (P)
00923.	41	<i>Hedbergella sigali</i> LO (PF)
00941.	7	<i>Hedbergella planispira</i> FO (PF)
00956.	304	M1r top (M)
00965.	195	<i>Conusphaera mexicana</i> LO (N)
00968.	261	<i>Phoberocysta neocomica</i> LO (P)
00973.	40	<i>Hedbergella sigali</i> FO (PF)
00983.	309	M4n top (M)
00991.	160	<i>Calicalathina oblongata</i> LO (N)
01008.	311	M5r top (M)
01018.	187	<i>Speetonia colligata</i> LO (N)
01028.	315	M7n top (M)
01056.	316	M7r top (M)
01057.	155	<i>Cruciellipsis cuvillieri</i> LO (N)
01073.	317	M8n top (M)
01074.	259	<i>Odontochitina operculata</i> FO (P)
	200	<i>Chiastozygus striatus</i> FO (N)
01090.	318	M8r top (M)
01099.	257	<i>Druggidium rhabdoreticulatum</i> FO (P)
01112.	321	M10n top (M)
01125.	322	M10r top (M)
01127.	189	<i>Tubodiscus verenae</i> LO (N)
01128.	323	M10Nn top (M)
01130.	156	<i>Cyclagelosphaera deflandrei</i> LO (N)
01138.	202	<i>Nannoconus bucheri</i> FO (N)
01143.	163	<i>Diadorhombus rectus</i> LO (N)
01149.	88	<i>Trochammina quinqueloba</i> LO (BF)
01167.	74	<i>Lenticulina nodosa</i> FO (BF)
	55	<i>Dorothia praehauteriviana</i> FO (BF)
01168.	324	M10Nr top (M)
01172.	325	M11n top (M)
01189.	203	<i>Parhabdolithus infinitus</i> FO (N)
01193.	262	<i>Scriniodinium dictyotum</i> LO (P)
01205.	255	<i>Druggidium deflandrei</i> FO (P)
01207.	204	<i>Diadorhombus rectus</i> FO (N)
01223.	185	<i>Reticulolithus wisei</i> LO (N)
01230.	188	<i>Tubodiscus verenae</i> FO (N)
	159	<i>Calicalathina oblongata</i> FO (N)
01243.	253	<i>Druggidium apicopaucicum</i> FO (P)
01253.	338	M15r top (M)
01264.	339	M16n top (M)
01269.	340	M16r top (M)
	206	<i>Reinhardtites fenestratus</i> FO (N)
01272.	208	<i>Speetonia colligata</i> FO (N)
01287.	251	<i>Biorbifera johnnewingii</i> FO (P)
01288.	190	<i>Vagapilla stradneri</i> FO (N)
01331.	184	<i>Reticulolithus wisei</i> FO (N)
01332.	68	<i>Haplophragmium inconstans</i> LO (BF)
01340.	173	<i>Nannoconus colomi</i> FO (N)
01350.	186	<i>Stephanolithion bigoti</i> LO (N)
01352.	67	<i>Haplophragmium inconstans</i> FO (BF)
01353.	171	<i>Lithraphidites carniolensis</i> FO (N)
01359.	154	<i>Cruciellipsis cuvillieri</i> FO (N)
01363.	78	<i>Lenticulina quenstedti</i> LO (BF)
01411.	158	<i>Conusphaera mexicana</i> FO (N)
01446.	87	<i>Trochammina quinqueloba</i> FO (BF)

2. DSDP Leg 93, Hole 603B, Western Atlantic Ocean.

Depth	Number	Fossil Name
01170.	263	<i>Spinidinium echinoideum</i> FO (P)
01188.	266	<i>Spinidinium vestitum</i> FO (P)
01205.	2	<i>Caucasella hoterivica</i> LO (PF)
01210.	256	<i>Druggidium deflandrei</i> LO (P)
01220.	7	<i>Hedbergella planispira</i> FO (PF)
01225.	304	M1r top (M)
01238.	261	<i>Phoberocysta neocomica</i> LO (P)
01255.	195	<i>Conusphaera mexicana</i> LO (N)
01292.	309	M4n top (M)
01300.	41	<i>Hedbergella sigali</i> LO (PF)

2. DSDP Leg 93, Hole 603B, Western Atlantic Ocean.

Depth	Number	Fossil Name
01307.	311	M5r top (M)
01320.	160	<i>Calicalathina oblongata</i> LO (N)
01324.	157	<i>Chiastozygus litterarius</i> FO (N)
01330.	187	<i>Speetonia colligata</i> LO (N)
01332.	315	M7n top (M)
01347.	254	<i>Druggidium apicopaucicum</i> LO (P)
01360.	155	<i>Cruciellipsis cuvillieri</i> LO (N)
01363.	316	M7r top (M)
01373.	259	<i>Odontochitina operculata</i> FO (P)
01381.	317	M8n top (M)
01384.	318	M8r top (M)
01387.	40	<i>Hedbergella sigali</i> FO (PF)
01404.	257	<i>Druggidium rhabdoreticulatum</i> FO (P)
01423.	321	M10n top (M)
01427.	156	<i>Cyclagelosphaera deflandrei</i> LO (N)
01433.	322	M10r top (M)
01436.	163	<i>Diadorhombus rectus</i> LO (N)
01446.	189	<i>Tubodiscus verenae</i> LO (N)
01447.	323	M10Nn top (M)
01469.	1	<i>Caucasella hoterivica</i> FO (PF)
01476.	262	<i>Scriniodinium dictyotum</i> LO (P)
01483.	324	M10Nr top (M)
01493.	325	M11n top (M)
01509.	71	<i>Lenticulina busnardoii</i> LO (BF)
	55	<i>Dorothia praehauteriviana</i> FO (BF)
01518.	255	<i>Druggidium deflandrei</i> FO (P)
01526.	159	<i>Calicalathina oblongata</i> FO (N)
01546.	185	<i>Reticulolithus wisei</i> LO (N)
01549.	253	<i>Druggidium apicopaucicum</i> FO (P)
01554.	338	M15r top (M)
01556.	188	<i>Tubodiscus verenae</i> FO (N)
01559.	339	M16n top (M)
01565.	204	<i>Diadorhombus rectus</i> FO (N)
01570.	208	<i>Speetonia colligata</i> FO (N)
01572.	340	M16r top (M)
01574.	251	<i>Biorbifera johnnewingii</i> FO (P)

3. DSDP Leg 44, Hole 391C, Western North Atlantic Ocean.

Depth	Number	Fossil Name
00784.	266	<i>Spinidinium vestitum</i> FO (P)
00926.	256	<i>Druggidium deflandrei</i> LO (P)
00927.	8	<i>Hedbergella trocoidea</i> FO (PF)
00963.	195	<i>Conusphaera mexicana</i> LO (N)
	176	<i>Rhagodiscus angustus</i> FO (N)
01009.	60	<i>Gavelinella barremiana</i> LO (BF)
01010.	196	<i>Nannoconus colomi</i> LO (N)
01012.	254	<i>Druggidium apicopaucicum</i> LO (P)
01019.	157	<i>Chiastozygus litterarius</i> FO (N)
	194	<i>Vagapilla matalosa</i> FO (N)
01030.	160	<i>Calicalathina oblongata</i> LO (N)
01031.	155	<i>Cruciellipsis cuvillieri</i> LO (N)
01091.	259	<i>Odontochitina operculata</i> FO (P)
01105.	197	<i>Nannoconus truitti</i> FO (N)
01126.	156	<i>Cyclagelosphaera deflandrei</i> LO (N)
01131.	257	<i>Druggidium rhabdoreticulatum</i> FO (P)
01137.	189	<i>Tubodiscus verenae</i> LO (N)
01147.	55	<i>Dorothia praehauteriviana</i> FO (BF)
	74	<i>Lenticulina nodosa</i> FO (BF)
01170.	202	<i>Nannoconus bucheri</i> FO (N)
01177.	255	<i>Druggidium deflandrei</i> FO (P)
01178.	185	<i>Reticulolithus wisei</i> LO (N)
01198.	188	<i>Tubodiscus verenae</i> FO (N)
	203	<i>Parhabdolithus infinitus</i> FO (N)
01199.	204	<i>Diadorhombus rectus</i> FO (N)
01210.	159	<i>Calicalathina oblongata</i> FO (N)
	206	<i>Reinhardtites fenestratus</i> FO (N)
01212.	253	<i>Druggidium apicopaucicum</i> FO (P)
01229.	190	<i>Vagapilla stradneri</i> FO (N)
01238.	184	<i>Reticulolithus wisei</i> FO (N)
01263.	251	<i>Biorbifera johnnewingii</i> FO (P)
01312.	171	<i>Lithraphidites carniolensis</i> FO (N)
01321.	173	<i>Nannoconus colomi</i> FO (N)
01372.	154	<i>Cruciellipsis cuvillieri</i> FO (N)

APPENDIX B (continued).

4. DSDP Leg 11, Site 105, Western Atlantic Ocean.

Depth	Number	Fossil Name
00306.	10	<i>Planomalina buxtorfi</i> LO (PF)
00307.	13	<i>Rotalipora appenninica</i> LO (PF)
00309.	263	<i>Spinidinium echoideum</i> FO (P)
00317.	12	<i>Rotalipora appenninica</i> FO (PF)
00322.	165	<i>Eiffellithus turriseiffeli</i> FO (N)
00388.	266	<i>Spinidinium vestitum</i> FO (P)
00392.	264	<i>Subtilisphaera perlucida</i> LO (P)
00404.	256	<i>Druggidium deflandrei</i> LO (P)
00426.	254	<i>Druggidium apicopaucicum</i> LO (P)
00430.	155	<i>Cruciellipsis cuvillieri</i> LO (N)
00433.	259	<i>Odontochitina operculata</i> FO (P)
00440.	257	<i>Druggidium rhabdoreticulatum</i> FO (P)
00457.	55	<i>Dorothia praehauteriviana</i> FO (BF)
00459.	262	<i>Scriniodinium dictyonum</i> LO (P)
00469.	74	<i>Lent icul ina nodosa</i> FO (BF)
00484.	255	<i>Druggidium deflandrei</i> FO (P)
00504.	253	<i>Druggidium apicopaucicum</i> FO (P)
00533.	251	<i>Biorbifera johnnewingii</i> FO (P)
00585.	186	<i>Stephanolithion bigotii</i> LO (N)
00603.	154	<i>Cruciellipsis cuvillieri</i> FO (N)

5. DSDP Leg 41, Site 370, Eastern Atlantic Ocean.

Depth	Number	Fossil Name
00674.	13	<i>Rotalipora appenninica</i> LO (PF)
	19	<i>Ticinella breggiensis</i> LO (PF)
	37	<i>Praeglobotruncana delrioensis</i> LO (PF)
00721.	32	<i>Hedbergella simplex</i> FO (PF)
	18	<i>Ticinella breggiensis</i> FO (PF)
	12	<i>Rotalipora appenninica</i> FO (PF)
00733.	165	<i>Eiffellithus turriseiffeli</i> FO (N)
00740.	36	<i>Praeglobotruncana delrioensis</i> FO (PF)
00816.	20	<i>Ticinella primula</i> FO (PF)
	8	<i>Hedbergella trocoidea</i> FO (PF)
00827.	264	<i>Subtilisphaera perlucida</i> LO (P)
00828.	7	<i>Hedbergella planispira</i> FO (PF)
	27	<i>Globigerinelloides blowi</i> LO (PF)
00829.	176	<i>Rhagodiscus angustus</i> FO (N)
	193	<i>Lithastrinus floralis</i> FO (N)
00840.	196	<i>Nannoconus colomii</i> LO (N)
	26	<i>Globigerinelloides blowi</i> FO (PF)
00876.	60	<i>Gavelinella barremiana</i> LO (BF)
00885.	259	<i>Odontochitina operculata</i> FO (P)
00889.	2	<i>Caucasella heterivica</i> LO (PF)
00891.	155	<i>Cruciellipsis cuvillieri</i> LO (N)
01120.	55	<i>Dorothia praehauteriviana</i> FO (BF)
01129.	74	<i>Lenticulina nodosa</i> FO (BF)
01139.	71	<i>Lenticulina busnardoii</i> LO (BF)
01140.	188	<i>Tubodiscus verenae</i> FO (N)
01158.	159	<i>Calcicalathina oblongata</i> FO (N)
01176.	190	<i>Vagapilla stradneri</i> FO (N)

6. DSDP Leg 77, Hole 535A, Western North Atlantic Ocean.

Depth	Number	Fossil Name
00160.	10	<i>Planomalina buxtorfi</i> LO (PF)
00326.	20	<i>Ticinella primula</i> FO (PF)
00368.	7	<i>Hedbergella planispira</i> FO (PF)
00401.	21	<i>Ticinella roberti</i> FO (PF)
00402.	261	<i>Phoberocysta neocomica</i> LO (P)
00403.	195	<i>Conusphaera mexicana</i> LO (N)
00404.	8	<i>Hedbergella trocoidea</i> FO (PF)
00421.	259	<i>Odontochitina operculata</i> FO (P)
00422.	157	<i>Chiastozygus litterarius</i> FO (N)
00444.	155	<i>Cruciellipsis cuvillieri</i> LO (N)
00459.	187	<i>Speetonia colligata</i> LO (N)
00478.	257	<i>Druggidium rhabdoreticulatum</i> FO (P)
00521.	200	<i>Chiastozygus striatus</i> FO (N)
00531.	189	<i>Tubodiscus verenae</i> LO (N)
00576.	163	<i>Diadorhombus rectus</i> LO (N)
00611.	203	<i>Parhabdolithus infinitus</i> FO (N)
00648.	188	<i>Tubodiscus verenae</i> FO (N)
00660.	71	<i>Lenticulina busnardoii</i> LO (BF)
00675.	206	<i>Reinhardites fenestratus</i> FO (N)
00684.	253	<i>Druggidium apicopaucicum</i> FO (P)

6. DSDP Leg 77, Hole 535A, Western North Atlantic Ocean.

Depth	Number	Fossil Name
00326.	20	<i>Ticinella primula</i> FO (PF)
00368.	7	<i>Hedbergella planispira</i> FO (PF)
00401.	21	<i>Ticinella roberti</i> FO (PF)
00402.	261	<i>Phoberocysta neocomica</i> LO (P)
00403.	195	<i>Conusphaera mexicana</i> LO (N)
00404.	8	<i>Hedbergella trocoidea</i> FO (PF)
00421.	259	<i>Odontochitina operculata</i> FO (P)
00422.	157	<i>Chiastozygus litterarius</i> FO (N)
00444.	155	<i>Cruciellipsis cuvillieri</i> LO (N)
00459.	187	<i>Speetonia colligata</i> LO (N)
00478.	257	<i>Druggidium rhabdoreticulatum</i> FO (P)
00521.	200	<i>Chiastozygus striatus</i> FO (N)
00531.	189	<i>Tubodiscus verenae</i> LO (N)
00576.	163	<i>Diadorhombus rectus</i> LO (N)
00611.	203	<i>Parhabdolithus infinitus</i> FO (N)
00648.	188	<i>Tubodiscus verenae</i> FO (N)
00660.	71	<i>Lenticulina busnardoii</i> LO (BF)
00675.	206	<i>Reinhardites fenestratus</i> FO (N)
00684.	253	<i>Druggidium apicopaucicum</i> FO (P)

7. DSDP Leg 50 , Hole 416A, Eastern Atlantic Ocean.

Depth	Number	Fossil Name
00730.	24	<i>Hedbergella delrioensis</i> FO (PF)
00764.	176	<i>Rhagodiscus angustus</i> FO (N)
00855.	7	<i>Hedbergella planispira</i> FO (PF)
00897.	157	<i>Chiastozygus litterarius</i> FO (N)
00900.	76	<i>Lenticulina ouachensis</i> LO (BF)
00982.	155	<i>Cruciellipsis cuvillieri</i> LO (N)
01118.	57	<i>Epistomina caracolla</i> LO (BF)
	96	<i>Dorothia praehauteriviana</i> LO (BF)
01188.	189	<i>Tubodiscus verenae</i> LO (N)
01198.	88	<i>Trochammina quinqueloba</i> LO (BF)
01199.	163	<i>Diadorhombus rectus</i> LO (N)
01204.	97	<i>Gavelinella barremiana</i> FO (BF)
01222.	71	<i>Lenticulina busnardoii</i> LO (BF)
01303.	74	<i>Lenticulina nodosa</i> FO (BF)
01361.	101	<i>Epistomina caracolla</i> FO (BF)
01391.	185	<i>Reticulolithus wisei</i> LO (N)
01400.	55	<i>Dorothia praehauteriviana</i> FO (BF)
01417.	100	<i>Lenticulina ouachensis</i> FO (BF)
01459.	70	<i>Lenticulina busnardoii</i> FO (BF)
01531.	188	<i>Tubodiscus verenae</i> FO (N)
	159	<i>Calcidalathina oblongata</i> FO (N)
01559.	171	<i>Lithraphidites carniolensis</i> FO (N)
01560.	184	<i>Reticulolithus wisei</i> FO (N)
01569.	56	<i>Epistomina uhligi</i> LO (BF)
01572.	173	<i>Nannoconus colomi</i> FO (N)
01615.	154	<i>Cruciellipsis cuvillieri</i> FO (N)
01616.	67	<i>Haplophragmium inconstans</i> FO (BF)
01624.	158	<i>Conusphaera mexicana</i> FO (N)

8. DSDP Leg 48A, Hole 398D, Eastern Atlantic Ocean.

Depth	Number	Fossil Name
00887.	164	<i>Eiffellithus eximus</i> FO (N)
00984.	22	<i>Ticinella roberti</i> LO (PF)
00993.	165	<i>Eiffellithus turriseiffeli</i> FO (N)
01250.	20	<i>Ticinella primula</i> FO (PF)
01311.	209	<i>Prediscosphaera cretacea</i> FO (N)
01345.	7	<i>Hedbergella planispira</i> FO (PF)
01468.	8	<i>Hedbergella trocoidea</i> FO (PF)
01487.	176	<i>Rhagodiscus angustus</i> FO (N)
01571.	193	<i>Lithastrinus floralis</i> FO (N)
01573.	196	<i>Nannoconus colomi</i> LO (N)
01591.	60	<i>Gavelinella barremiana</i> LO (BF)
01592.	157	<i>Chiastozygus litterarius</i> FO (N)
01598.	180	<i>Reticulolithus irregularis</i> FO (N)
01626.	160	<i>Calcidalathina oblongata</i> LO (N)
01697.	197	<i>Nannoconus truitti</i> FO (N)
01706.	194	<i>Vagapilla matalosa</i> FO (N)
01716.	155	<i>Cruciellipsis cuvillieri</i> LO (N)

APPENDIX B (continued).

9. DSDP Leg 41, Site 367, Eastern Atlantic Ocean.

Depth	Number	Fossil Name
00701.	36	<i>Praeglobotruncana delrioensis</i> FO (PF)
	8	<i>Hedbergella trocoidea</i> FO (PF)
00727.	165	<i>Eiffellithus turriseiffeli</i> FO (N)
00730.	20	<i>Ticinella primula</i> FO (PF)
	24	<i>Hedbergella delrioensis</i> FO (PF)
00787.	7	<i>Hedbergella planispira</i> FO (PF)
00891.	157	<i>Chiastozygus litterarius</i> FO (N)
	193	<i>Lithastrinus floralis</i> FO (N)
00897.	196	<i>Nannoconus colomii</i> LO (N)
00916.	160	<i>Calcicalathina oblongata</i> LO (N)
00940.	155	<i>Cruciellipsis cuvillieri</i> LO (N)
00941.	203	<i>Parhabdolithus infinitus</i> FO (N)
01024.	185	<i>Rucinolithus wisei</i> LO (N)
	204	<i>Diadorhombus rectus</i> FO (N)
01083.	184	<i>Rucinolithus wisei</i> FO (N)
01085.	171	<i>Lithaphidites carniolensis</i> FO (N)
	173	<i>Nannoconus colomii</i> FO (N)
01087.	154	<i>Cruciellipsis cuvillieri</i> FO (N)

10. DSDP Leg 43, Site 387, Western Atlantic Ocean.

Depth	Number	Fossil Name
00469.	165	<i>Eiffellithus turriseiffeli</i> FO (N)
00471.	209	<i>Prediscosphaera cretacea</i> FO (N)
00565.	256	<i>Druggidium deflandrei</i> LO (P)
00603.	195	<i>Conusphaera mexicana</i> LO (N)
00632.	160	<i>Calcicalathina oblongata</i> LO (N)
00633.	259	<i>Odontochitina operculata</i> FO (P)
	155	<i>Cruciellipsis cuvillieri</i> LO (N)
00642.	156	<i>Cyclagelosphaera deflandrei</i> LO (N)
00660.	257	<i>Druggidium rhabdoreticulatum</i> FO (P)
00735.	255	<i>Druggidium deflandrei</i> FO (P)
00746.	204	<i>Diadorhombus rectus</i> FO (N)
	185	<i>Rucinolithus wisei</i> LO (N)
00765.	159	<i>Calcicalathina oblongata</i> FO (N)
00772.	253	<i>Druggidium apicopaucum</i> FO (P)
00773.	188	<i>Tubodiscus verenae</i> FO (N)
00788.	190	<i>Vagapilla stradneri</i> FO (N)
00790.	251	<i>Biorbisera johnewingii</i> FO (P)

11. ODP Leg 123, Hole 765C, Eastern Indian Ocean.

Depth	Number	Fossil Name
00655.	267	<i>Diconodinium davidii</i> (P) FO
00665.	270	<i>Dingodinium cerviculum</i> (P) LO
	271	<i>Rhombodella paucispina</i> (P) LO
00683.	268	<i>Diconodinium davidii</i> (P) LO
00685.	221	<i>Prediscosphaera columnata</i> (N) FO
00703.	29	<i>Globigerinelloides ferreolensis</i> LO
00712.	7	<i>Hedbergella planispira</i> FO (PF)
00717.	220	<i>Hayesites irregularis</i> (N) FO
00721.	269	<i>Pseudoceratium turneri</i> (P) FO
	272	<i>Ascodinium</i> sp. A (P) PEAK
	24	<i>Hedbergella delrioensis</i> FO (PF)
	219	<i>Corolithion achyllosus</i> (N) FO
00724.	157	<i>Chiastozygus litterarius</i> FO (N)
00726.	216	<i>Eprolithus apertior</i> (N) FO
	217	<i>Eprolithus varoli</i> (N) FO
	218	<i>Flabellites biforaminis</i> (N) FO
	176	<i>Rhagodiscus angustus</i> FO (N)
00788.	301	M0r top (M)
00794.	303	M1n top (M)
00816.	259	<i>Odontochitina operculata</i> FO (P)
00833.	307	M3r top (M)
00845.	309	M4n top (M)
00863.	273	<i>Muderongia australis</i> (P) FO
	261	<i>Phoberocysta neocomica</i> LO (P)
00866.	189	<i>Tubodiscus verenae</i> LO (N)
00867.	215	<i>Tegumentum triples</i> (N) LO
00873.	155	<i>Cruciellipsis cuvillieri</i> LO (N)
	96	<i>Dorothia praealteriviana</i> LO (BF)
	94	<i>Gavelinella bettenstaedi</i> P (BF)
00882.	76	<i>Lenticulina ouachensis</i> LO (BF)
	92	<i>Paalzowella feifeli</i> LO (BF)
	93	<i>Epistomina caracolla</i> P (BF)

11. ODP Leg 123, Hole 765C, Eastern Indian Ocean.

Depth	Number	Fossil Name
00883.	185	<i>Rucinolithus wisei</i> LO (N)
00886.	213	<i>Tegumentum striatum</i> (N) LO
00891.	68	<i>Haplophragmium inconstans</i> LO (BF)
00892.	188	<i>Tubodiscus verenae</i> FO (N)
	212	<i>Tegumentum striatum</i> (N) FO
	214	<i>Tegumentum triples</i> (N) FO
00893.	184	<i>Rucinolithus wisei</i> FO (N)
	211	<i>Crucibiscutum salebrosum</i> (N) FO
	154	<i>Cruciellipsis cuvillieri</i> FO (N)
	55	<i>Dorothia praealteriviana</i> FO (BF)
00901.	89	<i>Verneuilinoides neocomiensis</i> LO (BF)
00903.	275	<i>Dissimilidinium ibispinosum</i> (P) LO
00904.	276	<i>Egmontodinium torynum</i> (P) P
00905.	274	<i>Batioladinium reticulatum</i> (P) P
00908.	88	<i>Trochammina quinqueloba</i> LO (BF)
00910.	91	<i>Pseudoreophax cisovnicensis</i> FO (BF)
00922.	95	<i>Hormosina cf. crassa</i> FO (BF)
00926.	90	<i>Verneuilinoides neocomiensis</i> FO (BF)
00928.	210	<i>Cyclagelosphaera deflandrei</i> (N) FO

12. ODP Leg 123, Site 766, Eastern Indian Ocean.

Depth	Number	Fossil Name
00253.	305	M2n top (M)
00259.	307	M3r top (M)
00272.	155	<i>Cruciellipsis cuvillieri</i> LO (N)
00290.	97	<i>Gavelinella barremiana</i> FO (BF)
00292.	72	<i>Lenticulina crepidularis</i> LO (BF)
00346.	317	M8n top (M)
00374.	319	M9n top (N)
00392.	98	<i>Conorboides hofkeri</i> FO (BF)
00400.	321	M10n top (M)
00422.	76	<i>Lenticulina ouachensis</i> LO (BF)
00425.	323	M10Nn top (M)
00434.	213	<i>Tegumentum striatum</i> (N) LO
00441.	325	M11n top (M)
00443.	189	<i>Tubodiscus verenae</i> LO (N)
00471.	214	<i>Tegumentum triples</i> (N) FO
	188	<i>Tubodiscus verenae</i> FO (N)
210		<i>Cyclagelosphaera deflandrei</i> (N) FO
212		<i>Tegumentum striatum</i> (N) FO
211		<i>Crucibiscutum salebrosum</i> (N) FO
154		<i>Cruciellipsis cuvillieri</i> FO (N)

13. DSDP Leg 27, Site 261, Eastern Indian Ocean.

Depth	Number	Fossil Name
00363.	301	M0r top (M)
00366.	303	M1n top (M)
00381.	305	M2n top (M)
00404.	307	M3r top (M)
00438.	309	M4n top (M)
00447.	155	<i>Cruciellipsis cuvillieri</i> LO (N)
00487.	188	<i>Tubodiscus verenae</i> FO (N)
00494.	68	<i>Haplophragmium inconstans</i> LO (BF)
	89	<i>Verneuilinoides neocomiensis</i> LO (BF)
00506.	206	<i>Reinhardtites fenestratus</i> FO (N)
00507.	154	<i>Cruciellipsis cuvillieri</i> FO (N)
00525.	88	<i>Trochammina quinqueloba</i> LO (BF)
00532.	208	<i>Speetonia colligata</i> FO (N)
	186	<i>Stephanolithion bigotii</i> LO (N)
	67	<i>Haplophragmium inconstans</i> FO (BF)
00549.	87	<i>Trochammina quinqueloba</i> FO (BF)
	90	<i>Verneuilinoides neocomiensis</i> FO (BF)
	78	<i>Lenticulina quenstedti</i> LO (BF)